ESA Support to Science Element

# Product Handbook for Ocean Heat Flux (OHF) Reference Dataset

ESA Contract No. 4000111424/14/I-AM

**1.0**

# STSE OHF

# Product Handbook for OHF Reference Dataset

| | |
|---|---|
| **Customer** | ESA / ESRIN |
| **Authors** | IFREMER, MIO |
| **ESRIN Contract Number** | 4000111424/14/I-AM |
| **Document Reference** | |
| **Version/Rev** | 1.0 |
| **Date of Issue** | 27 August 2015 |

| | | |
|---|---|---|
| **Prepared by/Lead Author (NHC)** | Abderrahim Bentamy | Signature |
| **Co-author** | Karina Von Schuckmann | |
| **Co-author** | Jean-François Piolle | |
| **Co-author** | Antoine Grouazel | |
| **Co-author** | Sergey Gulev | |
| **Co-author** | | |
| **Co-author** | | |
| **Co-author** | | |
| **Accepted by (ESA/ESRIN)** | | |

# Amendment history

| Version | Date | Change Description | Author |
|---|---|---|---|
| 1.0 | 27 August 2015 | Initial version | |

# Project team

| Name | Affeliation | Country |
|---|---|---|
| Abderrahim Bentamy* | IFREMER | France |
| Axel Andersson | DWD | Germany |
| Bertrand Chapron* | IFREMER | France |
| Carol Anne Clayson | WHOI | U.S. |
| Chris Merchant | UR | U.K |
| Clément de Boyer Montégut * | IFREMER | France |
| Frédéric Paul* | IFREMER | France |
| Igor Esau* | NERSC | Norway |
| Jean-François Piollé* | IFREMER | France |
| Johnny Johannessen* | NERSC | Norway |
| Josey Seymon | NOC | UK |
| Karina Von Schuchmann* | MIO | France |
| Keith Haines | UR | U.K |
| Nicolas Reul * | IFREMER | France |
| Pierre Philippe Mathieu | ESA technical officer | Italy |
| Rachel Pinker | DMUM | U.S |
| Rainer Hollmann | DWD | Germany |
| Rick Danielson* | NERSC | Norway |
| Hayley evers king* | PML | U.K |
| Semyon Grodsky | DMUM | U.S. |
| Sergey Gulev | IORAS | Russia |
| Shubha Sathyendranath* | PML | U.K |
| T. Platt* | PML | U.K |

## Summary

# 1 Introduction

## 1.1 Overview

This document aims at the description and characterization of the flux estimates collected (from IFREMER, HOAPS, OAFlux, SeaFlux, J-OFURO, CFSR, MERRA and ERA Interim) and standardized to build the OHF reference dataset It also provides further investigations of the quality of the standardization process.

This work was performed in the context of workpackage 2 of the OHF project, dealing with the homogenization of turbulent flux data derived from various satellite and numerical flux products.

The homogenization of available fluxes should be understood as a procedure aiming at the estimation of each product data on same grid map over global oceans. It should be read as standardization of the spatial and temporal resolutions as well as of data format. The resulting flux fields are available for the project and for users with unified spatial and temporal resolutions.

## 1.2 Applicable documents

The table list of the applicable documents to this document:

| Id | Title | Reference | Issue | Rev. |
|---|---|---|---|---|
| SOW | Statement of Work | EOP-SA/0261/PPM-ppm | 1 | 1. |

**Table 1: Applicable documents**

## 1.3 Reference documents

| Id | Title | Reference | Issue | Rev. |
|---|---|---|---|---|
| [RD-1] | Climate Data Guide | | | |

**Table 2: Reference documents**

## 1.4 Web resources

| Id | Title | Reference |
|---|---|---|
| [WEB-1] | OceanFlux GHG project climatology generator | http://www.ifremer.fr/cersat1/exp/oceanflux |
| [WEB-2] | Felyx software solution | http://felyx.org |
| [WEB-3] | Ifremer/Cersat | http://cersat.ifremer.fr/ |
| [WEB-4] | HOAPS | http://www.hoaps.zmaw.de/ |
| [WEB-5] | OAFlux | http://oaflux.whoi.edu/data.html |
| [WEB-6] | SeaFlux | http://seaflux.org/ |
| [WEB-7] | J-OFURO | http://dtsv.scc.u-tokai.ac.jp/j-ofuro/ |
| [WEB-8] | NOCS2 | http://noc.ac.uk/science-technology/earth-ocean-system/atmosphere-ocean/noc-surface-flux-dataset |
| [WEB-9] | ERA Interim | http://www.ecmwf.int/en/research/climate-reanalysis/era-interim |
| [WEB-10] | CFSR | https://climatedataguide.ucar.edu/climate-data/climate-forecast-system-reanalysis-cfsr |
| [WEB-11] | JPL QuikSCAT L2B 12.5 km data | podaac.jpl.nasa.gov/OceanWinds/quikscat/preview/L2B12/v3/ |
| [WEB-12] | Ifremer/cersat wave data | ftp://ftp.ifremer.fr/ifremer/cersat/products/swath/altimeters/waves/documentation/ |
| [WEB-13] | Oceansites | http://www.oceansites.org |
| [WEB-14] | SAMOS | http://samos.coaps.fsu.edu/html/ |

**Table 3: Web resources**

## 1.5 Scientific publications

| | |
|---|---|
| [SP-1] | Ayina L. H., A. Bentamy, A. Mestas-Nunez, G. Madec, 2006: The impact of satellite winds and latent heat fluxes in a numerical simulation of the tropical Pacific Ocean. Journal of Climate, 19(22), 5889-5902. http://dx.doi.org/10.1175/JCLI3939.1 |

| | |
|---|---|
| [SP-2] | Andersson A., K. Fennig, C. Klepp, S. Bakan, H. Graßl, and J. Schulz, 2010: The Hamburg Ocean Atmosphere Parameters and Fluxes from Satellite Data - HOAPS-3, Earth System Science. Data, 2, 215-234, doi:10.5194/essd-2-215-2010.1 |
| [SP-3] | Andersson, A., Klepp, C., Fennig, K., Bakan, S., Grassl, H., & Schulz, J. , 2011: Evaluation of HOAPS-3 ocean surface freshwater flux components. Journal of Applied Meteorology and Climatology, 50, 379-398. |
| [SP-4] | Bentamy, A., P. Queffeulou,, Y. Quilfen, K. Katsaros,1999: Ocean surface wind fields estimated from satellite active and passive microwave instruments, IEEE T. Geoscience and Remote Sensing, 37 (5) , 2469-2486 |
| [SP-5] | Bentamy A., K B. Katsaros, M. Alberto, W. M. Drennan, E. B. Forde, 2002: Daily surface wind fields produced by merged satellite data. American Geophys. Union, Geophysical Monograph Series Vol. 127, 343-349. |
| [SP-6] | Bentamy, A., K. B. Katsaros, A. M. Mestas-Nuñez, W. M. Drennan, E. B. Forde and H. Roquet, 2003. Satellite estimates of wind speed and latent heat flux over the global oceans. J. Climate, 16, 637-656. |
| [SP-7] | Bentamy, A., H.-L. Ayina, P. Queffeulou, and D. Croize-Fillon ,2007: Improved Near Real Time Surface Wind Resolution over The Mediterranean Sea, Ocean Sci., 3, 259-271. |
| [SP-8] | Bentamy, A., L-H. Ayina, W. Drennan, K. Katsaros, A. M. Mestas-Nuñez, and R. T. Pinker, 2008. 15 years of ocean surface momentum and heat fluxes from remotely sensed observations, FLUXNEWS, 5, World Climate Research Programme, Geneva, Switzerland, 14–16 (http://sail.msk.ru/newsletter/fluxnews_5_final.pdf). |
| [SP-9] | Bentamy, A., D. Croize-Fillon, and C. Perigaud , 2008: Characterization of ASCAT measurements based on buoy and QuikSCAT wind vector observations, Ocean Sci., 4, 265–274. |
| [SP-10] | *Bentamy A., D. Croizé. Fillon, 2011:* Gridded Surface Wind Fields from Metop/ASCAT Measurements. International Journal of Remote Sensing, 33, pp 1729-1754. |
| [SP-11] | BENTAMY, A., S. A. GRODSKY, J. A. CARTON, D. CROIZÉ-FILLON, AND B. CHAPRON, 2012: MATCHING ASCAT AND QUIKSCAT WINDS, J. GEOPH. RES., 117, C02011, DOI:10.1029/2011JC007479. |
| [SP-12] | Bentamy, A., S. A. Grodsky, K. Katsaros, A. M. Mestas-Nuñez, B. Blanke and F. Desbiolles , 2013: Improvement in air–sea flux estimates derived from satellite observations, International Journal of Remote Sensing, 34 (14), DOI:10.1080/01431161.2013.787502. |
| [SP-13] | Bentamy A., Grodsky S. A., Chapron B., Carton J. A., 2013: Compatibility of C- and Ku-band scatterometer winds: ERS-2 and QuikSCAT. J. Marine System 117-118, 72-80 |
| [SP-14] | Berg, W., C. Kummerow, M. Sapiano, N. Rodriguez-Alvarez, and F. Weng, A Fundamental Climate Data Record of Microwave Brightness Temperature data from 25 Years of SSM/I and SSMIS Observations, GEWEX Newsletter, August 2012. |
| [SP-15] | Berry, D.I. and E.C. Kent, 2011, Air-sea fluxes from NOCS2.0: the construction of a new gridded dataset with uncertainty estimates. International Journal Climatology. (CLIMAR-III Special Issue), 31, 987-1001 (doi:10.1002/joc.2059). |
| [SP-16] | Bretherton, F.P., D.M. Burrige, J. Crease, F.W. Dobson, E.B. Kraus and T.H. Vander Haar , 1982: The CAGE experiment, a feasibility study, UNESCO report. |
| [SP-17] | Bradley, E. F. and C.W Fairall, 2007: A Guide to Making Climate Quality Meteorological and Flux Measurements at Sea. NOAA Technical Memorandum OAR PSD-311, NOAA/ESRL/PSD, Boulder, CO, 108 pp. |
| [SP-18] | Chou, S.-H., E. Nelkin, J. Ardizzone, R. M. Atlas, and C.-L. Shie, 2003: Surface turbulent heat and momentum fluxes over global oceans based on the Goddard satellite retrieval, |

| | |
|---|---|
| | version 2 (GSSTF2). Journal of Climate, 16, 3256–3273. |
| [SP-19] | Fairall, C. W., T. Uttal, D. Hazen, J. Hare, M. F. Cronin, N. Bond, and D. E. Veron, 2007: Observations of Cloud, Radiation, and Surface Forcing in the Equatorial Eastern Pacific. J. Climate, Volume 21, Issue 4 (February 2008) pp. 655-673 doi: http://dx.doi.org/10.1175/2007JCLI1757.1 |
| [SP-20] | Fairall, C. W., M. Yang, L. Bariteau, J. B. Edson, D. Helmig, W. McGillis, S. Pezoa, J. E. Hare, B. Huebert, and B. Blomquist, 2011: Implementation of the COARE algorithm with O3, CO2 and DMS. J. Geophys. Res., 116, C00F09, doi:10.1029/2010JC006884. |
| [SP-21] | Fennig, K., Andersson, A., Bakan, S., Klepp, C., Schroeder, M., 2012: Hamburg Ocean Atmosphere Parameters and Fluxes from Satellite Data - HOAPS 3.2 - Monthly Means / 6-Hourly Composites. Satellite Application Facility on Climate Monitoring. doi:10.5676 / EUM_SAF_CM / HOAPS / V001. |
| [SP-22] | Fennig, Karsten; Andersson, Axel; Schröder, Marc (2013): Fundamental Climate Data Record of SSM/I Brightness Temperatures - . Satellite Application Facility on Climate Monitoring. DOI:10.5676/EUM_SAF_CM/FCDR_SSMI/V001 http://dx.doi.org/10.5676/EUM_SAF_CM/FCDR_SSMI/V001 |
| [SP-23] | Gulev, S.K., T. Jung, and E. Ruprecht, 2007: Estimation of the impact of sampling errors in the VOS observations on air-sea fluxes. Part II. Impact on trends and interannual variability. J. Climate, 20, 302-315. |
| [SP-24] | Gulev, S.K. and coauthors, 2010: Surface energy and CO2 fluxes and sea ice for ocean monitoring and prediction. ESA special volume on OceanObs'09 Plenary White Paper at Oceanobs-09, Venice, Italy, September 2010. |
| [SP-25] | Gulev, S.K., and K.P. Belyaev, 2012: Probability distribution characteristics for surface air-sea turbulent heat fluxes over the global ocean. J. Climate, 25, 184-206, 2012, doi: 10.1175/2011JCLI4211.1 |
| [SP-26] | Gulev SK, Latif M, Keenlyside N, Park W, Koltermann KP , 2013: North Atlantic Ocean control on surface heat flux on multidecadal timescales. Nature, 499, 464–467. |
| [SP-27] | Kubota, M., and H. Tomita, 2007: Introduction of J-OFURO latent heat flux version 2. Proc. Joint 2007 EUMETSAT Meteorological Satellite Conf. and 15th Satellite Meteorology and Oceanography Conf., Amsterdam, Netherlands, EUMETSAT and Amer. Meteor. Soc. |
| [SP-28] | Klepp, C., Andersson, A., & Bakan, S. (2008). The HOAPS climatology: Evaluation of latent heat flux. Newsletter of the WCRP Working Group on Surface Fluxes, 5, 30-32. |
| [SP-29] | Pinker, R. T., H. Wang, and S. A. Grodsky, 2009. How good are ocean buoy observations of radiative fluxes? Geophys. Res. Lett., 36, L10811, doi:10.1029/2009GL037840. |
| [SP-30] | Pinker R. T., A. Bentamy, K. B. Katsaros, Y. Ma, and C. Li, 2014: Estimates of net heat fluxes over the Atlantic Ocean. J. Geophy. Res. VOL. 119, 1–18, doi:10.1002/2013JC009386, 2014 |
| [SP-31] | Sathyendranath, S, Gouveia, AD, Shetye, SR, Ravindran, P, Platt, T (1991) Biological control of surface temperature in the Arabian Sea. Nature 349: 54-56. |
| [SP-32] | Tomita,H. and M. Kubota, 2006: An analysis of the accuracy of Japanese Ocean Flux data sets with Use of Remote sensing Observations(J-OFURO) satellite-derived latent heat flux using moored buoy data, Journal of Geophysical Research, 111, C07007, doi:10,1029/2005 JC003013, 2006. |
| [SP-33] | WCRP, 2013: Report from the World Climate Research Program (WCRP). May 2013 (http://www.wmo.int/pages/prog/sat/meetings/documents/ET-SUP-7_Doc_08-03_WCRP.pdf) |
| [SP-34] | Von Schuckmann, K., Gaillard, F., and Le Traon, P. Y., 2009: Global hydrographic variability patterns during 2003–2008, J. Geophys. Res., 114, C09007, |

| | |
|---|---|
| | doi:10.1029/2008JC005237. |
| [SP-35] | Von Schuckmann, K. and Le Traon, P.-Y.: How well can we derive Global Ocean Indicators from Argo data?, Ocean Sci., 7, 783–791, doi:10.5194/os-7-783-2011, 2011. |
| [SP-36] | Von Schuckmann, K., J.-B. Sallée, D. Chambers, P.-Y. Le Traon, C. Cabanes, F. Gaillard, S. Speich, M. Hamon, 2014: Monitoring ocean heat content from the current generation of global ocean observing systems, Ocean Sci. Discuss., 10, 923-949, www.ocean-sci-discuss.net/10/923/2013/, doi:10.5194/osd-10-923-2013 |
| [SP-37] | Valdivieso, M. and Co-authors (2014) Heat fluxes from ocean and coupled reanalyses. Clivar Exchanges Issue 64, 28-31. |
| [SP-38] | WCRP, 2013: Report from the World Climate Research Program (WCRP). May 2013 (http://www.wmo.int/pages/prog/sat/meetings/documents/ET-SUP-7_Doc_08-03_WCRP.pdf) |
| [SP-39] | Wentz, F. J., (2013), "SSM/I Version-7 Calibration Report", report number 011012, Remote Sensing Systems, Santa Rosa, CA, 46pp. |
| [SP-40] | WGASF, 2000: Intercomparison and validation of ocean-atmosphere energy flux fields - Final report of the Joint WCRP/SCOR Working Group on Air-Sea Fluxes. WCRP-112, WMO/TD-1036. P. K. Taylor, Ed., 306 pp., http://eprints.soton.ac.uk/69522/1/wgasf_final_rep.pdf |
| [SP-41] | WOAP, 2012: Report action plan for WCRP activities on surface fluxes, WCRP informal report (http://www.wcrp-climate.org/documents/woap_fluxes_report_01_2012.pdf) |
| [SP-42] | Yu, L., X. Jin, and R.A. Weller, 2007: Annual, seasonal, and interannual variability of air–sea heat fluxes in the Global Ocean. Journal of Climate, 20, 3190-3209, doi: 10.1175/JCLI4163.1. |
| [SP-43] | Yu, L., X. Jin, and R. A. Weller, 2008: Multidecade global flux datasets from the objectively analyzed air–sea fluxes (OAFlux) project: Latent and sensible heat fluxes, ocean evaporation, and related surface meteorological variables. Tech. Rep. OA- 2008-01, Woods Hole Oceanographic Institution, OAFlux Project, 64 pp. |
| [SP-44] | Zhai, L, Tang C, Platt, T, Sathyendranath, S (2011) Ocean response to attenuation of visible light by phytoplankton in the Gulf of St. Lawrence, J. Mar. Syst., doi:10.1016/j.jmarsys.2011.05.005 |
| [SP-45] | Fore A., B. Stiles, R. S. Dunbar, B. Williams, A. Chau, L. Ricciardulli, F. Wentz, T. Meissner and E. Rodridguez, 2011: Point-wise wind retrieval and ambiguity removal improvements for the QuikSCAT climatological data set. International Ocean Vector Wind Science Team Meeting Annapolis, Maryland, USA, 9-11 May 2011 (http://coaps.fsu.edu/scatterometry/meeting/past.php#2011) |
| [SP-46] | Ricciardulli L. and F. Wentz, 2011: Reprocessed QuikSCAT (V04) wind vectors with Ku-2011 geophysical model function. Remote Sensing Systems Technical Report 043011 (http://www.ssmi.com/qscat/qscat_Ku2011_tech_report.pdf) |
| [SP-47] | Reynolds, R.W., T.M. Smith, C. Liu, D.B. Chelton, K.S. Casey, M.G. Schlax (2007), Daily High-Resolution-Blended Analyses for Sea Surface Temperature. J. Climate, 20, 5473-5496. |
| [SP-48] | Jackson, D.L.,and G.A. Wick, 2010: Near-surface air temperature retrieval derived from AMSU-A and sea surface temperature observations. J. Atmos. Oceanic Technol., 27, 1769-1776. |
| [SP-49] | Queffeulou P. et D. Croizé-Fillon, Global altimeter SWH data set, version 11, June 2014. Ifremer technical report, available at :ftp://ftp.ifremer.fr/ifremer/cersat/products/swath/altimeters/waves/documentation/ |
| [SP-50] | Chou, S.-H., E. Nelkin, J. Ardizzone, R. M. Atlas, and C.-L. Shie, 2003: Surface turbulent heat and momentum fluxes over global oceans based on the Goddard satellite retrieval, |

| | |
|---|---|
| | version 2 (GSSTF2). Journal of Climate, 16, 3256–3273. |
| [SP-51] | Simmons A, Uppala S, Dee D, Kobayashi S. 2006. ERA-Interim: New ECMWF reanalysis products from 1989 onwards. ECMWF Newsletter 110 : 26 – 35. |
| [SP-52] | Fairall, C.W., E.F Bradley, J.E. Hare, A.A. Grachev, and J.B. Edson , 2003: Bulk parameterization of air-sea fluxes: updates and verification for the COARE3.0 algorithm, J. Climate, 16, 571-591. |
| [SP-53] | Desbiolles Fabien, Blanke Bruno, Bentamy Abderrahim, Grima Nicolas (2014). Origin of fine-scale wind stress curl structures in the Benguela and Canary upwelling systems. Journal Of Geophysical Research-oceans, 119(11), 7931-7948. http://dx.doi.org/10.1002/2014JC010015 |
| [SP-54] | Desbiolles Fabien, Blanke Bruno, Bentamy Abderrahim (2014). Short-term upwelling events at the western African coast related to synoptic atmospheric structures as derived from satellite observations. Journal Of Geophysical Research-oceans, 119(1), 461-483. Publisher's official version : http://dx.doi.org/10.1002/2013JC009278 , Open Access version : http://archimer.ifremer.fr/doc/00172/28333/ |
| [SP-55] | Kummerow C., W. Berg, M. Sapiano, N. Rodriguez-Alvarez, F. Weng, 2013. A Fundamental Climate Data Record of Intercalibrated Brightness Temperature Data from SSM/I and SSMIS. CDR Team Meeting July 30 – Aug 1, 2013. |
| [SP-56] | Sapiano, M. R. P., W. K. Berg, D. S. McKague, and C. D. Kummerow, 2012: Toward an Intercalibrated Fundamental Climate Data Record of the SSM/I Sensors. IEEE Trans. Geosci. Rem. Sens., Vol. 51 , Issue 3, doi 10.1109/TGRS.2012.2206601 |
| [SP-57] | Grodsky, S. A., V. N. Kudryavtsev, A. Bentamy, J. A. Carton, and B. Chapron, 2012. Does direct impact of SST on short wind waves matter for scatterometry?, Geophys. Res. Lett. 39, L12602, DOI: 10.1029/2012GL052091. |
| [SP-58] | Clayson, C. A., J. B. Roberts, and A. Bogdanoff, 2013: SeaFlux Version 1: a new satellite-based ocean-atmosphere turbulent flux dataset. *International Journal of Climatology*, in revision. |
| [SP-59] | Roberts, J. B., C. A. Clayson, F. R. Robertson, and D. Jackson, 2010: Predicting near - surface characteristics from SSM/I using neural networks with a first guess approach. J. Geophys. Res. , 115 , D19113, doi: 10.1029/2009JD013099 |
| [SP-60] | Schlussel, P., L. Schanz, and G. Englisch (1995), Retrieval of latent-heat flux and longwave irradiance at the sea-surface from SSM/I and AVHRR measurements, Adv. Space Res. , 16 , 107–116, doi:10.1016/0273- 1177(95)00389-V. |
| [SP-61] | Tomita, H. and M. Kubota, 2006: An analysis of the accuracy of Japanese Ocean Flux data sets with Use of Remote sensing Observations (J-OFURO) satellite-derived latent heat flux using moored buoy data,J. Geophys. Res, 111, C07007, doi:10,1029/2005 JC003013, 2006. |
| [SP-62] | Kurihara, Y., T. Sakurai, and T. Kuragano, 2006: Global daily sea surface temperature analysis using data from satellite microwave radiometer, satellite infrared radio meter and in-situ observations (in Japanese), Weather Bull., 73 , s1–s18. |
| [SP-63] | Fairall CW, Bradley EF, Hare JE, Grachev AA, Edson JB. 2003.Bulk parameterization of air–sea fluxes: updates and verification for the COARE algorithm. Journal of Climate 16: 571–591, DOI:10.1175/1520- 0442(2003)016<0571:BPOASF>2.0.CO;2. |
| [SP-64] | Chou, S.-H., E. Nelkin, J. Ardizzone, and R.M. Atlas, 2004: A comparison of latent heat fluxes over global oceans for four flux products, J. Climate, 17, 3973-3989. |
| [SP-65] | Wentz, F. J, 1997: A well calibrated ocean algorithm for special sensor microwave/imager, J. Geophys. Res.,102(C4), 8703–8718. |
| [SP-66] | Saha S et al (2010) The NCEP climate forecast system reanalysis. Bull Am Met Soc 91:1015– |

| | |
|---|---|
| | 1057 |
| [SP-67] | Andersson, E. and Järvinen, H., 1999: Variational quality control. Q. J. R. Meteorol. Soc., 125, 697-722 |
| [SP-68] | Bosilovich, M. G., cited, 2008: NASA's modern era retrospective analysis for research and applications: Integrating Earth observations. Earthzine. ( http://www.earthzine.org/2008/09/26/nass as modern-era-retrospective-analysis/) |
| [SP-69] | Rienecker, M. M., and Coauthors, 2011: MERRA: NASA's Modern-Era Retrospective Analysis for Research and Applications. J. Climate, 24, 3624–3648 |
| [SP-70] | Lock, A. P., A. R. Brown, M. R. Bush, G. M. Martin, and R. N. B. Smith, 2000: A new boundary layer mixing scheme. Part I: Scheme description and single-column model tests. Mon. Wea. Rev., 128, 3187–3199. |
| [SP-71] | Louis, J. F., M. Tiedtke, and J. Geleyn, 1982: A short history of the operational PBL parameterization at ECMWF. Proc. Workshop on Planetary Boundary Layer Parameterization, Reading, United Kingdom, ECMWF, 59–80. |
| [SP-72] | Charnock, H.: Wind-stress on a water surface, Q. J. Roy. Meteorol. Soc., 81, 639–640, 1955 |
| [SP-73] | Beljaars, A. C. M., 1995: The parametrization of surface fluxes in large-scale models under free convection. Q.J.R. Meteorol. Soc., 121: 255–270. doi: 10.1002/qj.49712152203 |
| [SP-74] | Smith, S. D. 1980 :Wind Stress and Heat Flux over the Ocean in Gale Force Winds, J. Phys. Oceanogr. 10: 709–726. |
| [SP-75] | Smith, Stuart D. 1988: Coefficients for Sea Surface Wind Stress, Heat Flux, and Wind Profiles as a Function of Wind Speed and Temperature, Journal of Geophysical Research 93 (C12): 15467. doi:10.1029/JC093iC12p15467 |


**Table 4: Scientific publications**

## 75.1 Abbreviations and Acronyms

| | |
|---|---|
| AATSR | Advanced Along Track Scanning Radiometer (ESA instrument) |
| ADB | Actions Data Base |
| AMSRE | Advanced Microwave Scanning Radiometer – E (of NASA's EoS Aqua) |
| API | Application Programming Interface |
| ATSR-1 | Along Track Scanning Radiometer onboard ERS-1 (ESA instrument) |
| ATSR-2 | Along Track Scanning Radiometer onboard ERS-2 (ESA instrument) |
| AMSR-E | Advanced Microwave Scanning Radiometer for EOS (NASA instrument) |
| AOD | Aerosol optical thickness |
| AOT | Aerosol optical depth |
| ASAR | Advanced Synthetic Aperture Radar |
| ASCAT | Advanced SCATterometer (of MetOp) |

| | |
|---|---|
| ATBD | Algorithm theoretical basis document |
| AVHRR | Advanced Very High Resolution Radiometer (NOAA instruments) |
| CCI | Climate Change Intiative |
| CDR | Critical Design Review |
| CEOS | Committee on Earth Observation Satellites |
| CERSAT | Centre de Recherche et d'Exploitation Satellitaire (IFREMER Satellite Data Center) |
| CLIVAR | Climate and Variability |
| DARD | Data Access and Requirements Document |
| DIR | Directory |
| DMSP | Defense Meteorological Satellite Program (of the USA) |
| DVP | Development and Validation Plan |
| DWD | Deutscher Wetterdienst |
| ECMWF | European Centre for Medium-Range Weather Forecasts |
| ENVISAT | Environment Satellite |
| EO | Earth observation |
| EOS | Earth Observing System |
| ERS | European Remote Sensing satellite (ESA instrument) |
| ERSEM | European Regional Seas Ecosystem Model |
| ESA | European Space Agency |
| EU | European Union |
| EUMETSAT | European Organisation for the Exploitation of Meteorological Satellites |
| FOAM | Forecast Ocean Assimilation Model |
| FR | Final Report |
| FP | Final Presentation |
| FTP | File transfer protocol |
| GCOS | Global Climate Observing System |
| GHRSST | Group for High Resolution Sea Surface Temperature |
| GMES | Global Monitoring for Environment and Security |
| GOCE | Gravity field and steady-state Ocean Circulation Explorer |
| GSICS | Global Space-based Inter-Calibration System |
| Hs | Significant Wave Height (also SWH) |
| ICD | Interface Control Document |
| IFREMER | Institut Français de Recherche pour l'Exploitation de la Mer |
| IOCCG | International Ocean Colour Coordinating Group |
| IOWAGA | Integrated Ocean Waves for Geophysical and other Application |
| IOVWST | International Ocean Vector Wind Science Team |
| IR | Infra-red (a piece of the electromagnetic spectrum) |
| ITT | Invitation To Tender |
| Jason-1 | Altimetry mission (NASA/France instrument) |
| Jason-2 | Altimetry mission (NASA/France instrument) |
| HOAPS | Hamburg Ocean Atmosphere Parameters and Fluxes from Satellite Data |
| KO | Kick Off |

| | |
|---|---|
| LHF | Latent Heat Flux |
| LW | Long Wave |
| MERIS | Medium Resolution Imaging Spectrometer (ESA instrument) |
| MODIS | Moderate Resolution Imaging Spectrometer (NASA instrument) |
| MR | Monthly Report |
| NASA | National Aeronautics and Space Administration (US) |
| NCDC | National Climatic Data Center |
| NERC | UK Natural Environment Research Council |
| NetCDF | Network Common Data Form |
| NetCDF CF | NetCDF Climate and Forecast Metadata Convention |
| NOAA | National Oceanographic and Atmospheric Administration (US) |
| NOC | National Oceanography Centre (UK) |
| NOP | Numerical Ocean Prediction |
| NPOESS | National Polar-orbiting Operational Environmental Satellite System |
| NRT | Near Real Time |
| NTC | Non Time Critical |
| NWP | Numerical Weather Prediction |
| NWC | Numerical Weather nowCasting |
| OAFlux | Ocean Atmosphere Flux |
| OC | Ocean colour |
| OC-flux | ESA STSE project – Open ocean and Coastal CO2 fluxes in support of carbon cycle monitoring |
| OHF | Ocean Heat Flux |
| OPeNDAP | Open-source Project for a Network Data Access Protocol |
| OSTIA | Operational Sea Surface Temperature and Sea Ice Analysis (UK Meteorological Office) |
| PaaS | Platform as a Service |
| PAR | Preliminary analysis report |
| PI | Principal Investigator |
| PML | Plymouth Marine Laboratory |
| PR | Progress Report |
| PMR | Passive Microwave Radiometry |
| RA2 | Radar altimeter 2 (ESA instrument) |
| RB | Requirements Baseline |
| RD | Reference Document |
| RRS | Remote Sensing Reflectance |
| RUG | Reference User Group |
| SaaS | Software as a Service |
| SAP | Scientific Analysis Plan |
| SAR | Scientific Assessment Report |
| SAR | Synthetic Aperture RADAR |
| SeaWIFS | Sea-viewing Wide Field-of-view Sensor |
| SEVIRI | Spinning Enhanced Visible and Infrared Imager (of Meteosat Second Generation) |

| | |
|---|---|
| SIAR | Scientific and Impact Assessment Report |
| SOLAS | Surface Ocean and Lower Atmosphere Study |
| SoW | HR-DD Statement of Work |
| SR | Scientific Roadmap |
| SRR | System Requirements Review |
| SSH | Sea Surface Height |
| SSM/I | Special Sensor Microwave Imager (of DMSP) |
| SSS | Sea Surface Salinity |
| SST | Sea Surface Temperature |
| SST-VC | SST Virtual Constellation (of CEOS) |
| STSE | Support to Science Element |
| TBC | To Be Confirmed |
| TBD | To Be Determined |
| TDP | Technical Data Package |
| TDS | Test Data Set |
| TN | Technical Note (short report 10-50 pages) |
| TO | Technical Officer (of the Agency) |
| TOA | Top of Atmosphere |
| TR | Technical Report (long report > 50 pages) |
| TS | Technical Specification |
| TOPEX | TOPEX-Poseidon altimetry mission (NASA/France) |
| UM | User Manual |
| URL | Universal Resource Locator |
| VIIRS | The NOAA Visible Infrared Imager Radiometer Suite |
| WCRP | World Climate Research Programme |
| WGASF | Working Group on Air-Sea Fluxes |
| WHOI | Woods Hole Oceanographic Institute |
| WGSF | Working Group on Surface Fluxes |
| WP | Work package |
| 1D | One dimensional |
| 3D | Three dimensional |

**Table 5: List of abbreviations and acronyms**

# 2 Data description

Table 6 summarizes the main characteristics of flux products (turbulent and radiative fluxes, and the associated bulk variables) used to meet the requirements. Four types of data, available over global ocean, are considered. Fluxes estimated based only on remotely sensed observations such as IFREMER (Institut Français pour la Recherche et l'Exploitation de la MER; France), HOAPS (Hamburg Ocean Atmosphere Parameters and Fluxes from Satellite; Germany), SeaFlux (Woods Hole Oceanographic Institution, Woods Hole (WHOI); USA), and J-OFURO (Japanese Ocean Flux Data sets with Use of Remote Sensing Observations; Japan). Fluxes estimated as blended products such as OAFlux (Objectively Analyzed air-sea Flux (WHOI); USA). The third kind of flux product is derived from numerical weather predictions centers. In this project the reanalysis performed and provided by the European Centre of Medium Weather Forecasts (ECMWF), named ERA Interim, and by the National Center for Environmental Prediction (NCEP) known as Climate Forecast System Reanalysis (CFSR) are used. Flux data determined from *Voluntary Observing Ship (VOS) measurements as daily analysis are processed and provided by* National Oceanography Centre Southampton and referred as NOCS2.

Only IFREMER, HOAPS, OAFlux, SeaFlux, J-OFURO, and ERA Interim products are used to assess the quality of the methods aiming at the calculation of the "standardized" flux products.

## 2.1 IFREMER

In this study we use the new version of the IFREMER turbulent flux estimates (Bentamy et al., 2014) at daily time scale over global oceans at a spatial resolution of 0.25° in longitude and latitude. It is an updated version of [SP12]. The bulk variables such as surface wind speed (W10) and specific air humidity (Qa10) at 10 m height are estimated from remotely sensed observations. W10 is obtained from the SeaWind scatterometer on board QuikSCAT satellite. More specifically, this project uses new QuikSCAT wind retrievals indicated as QuikSCAT V3 (ftp://podaac.jpl.nasa.gov/OceanWinds/quikscat/preview/L2B12/v3/). They are made available by Jet Propulsion Laboratory (JPL)/ Physical Oceanography. Distributed Active Archive Center (PODAAC) scientific team [SP45]. The new QuikSCAT V3 products are calculated based on the use of a geophysical model function ensuring the consistency with winds retrieved from microwave radiometers such as Special Sensor Microwave Imager (SSM/I) and WindSat [SP48]. Wind retrievals are provided over QuikSCAT swath at Wind Vector Cell (WVC) of 12.5km spatial resolution. This new scatterometer product is assumed improving wind speed performance in rain and at high wind speed conditions.

Specific air humidity is derived, over special sensor microwave imager (SSM/I) radiometer swaths , based on the use of the model relaying brightness temperature measurements (Tb) and Qa10 [SP12]. SSM/I are onboard the polar orbiting satellites DMSP F10, F11, F13, F14, and F15. For this project, a new reprocessing

of Qa10 is performed with respect to the use of the recently reprocessed fundamental climate data record (FCDR) brightness temperatures [SP55]. The latter are produced by the Colorado State University [SP56] with NOAA funding support.

Air and sea surface temperatures required for flux calculation are derived from ERA-Interim re-analyses (www.ecmwf.int/en/research/climate-reanalysis/era-interim) and from the Reynolds Optimally Interpolated version 2 (named hereafter NOAA SST) (http://www.ncdc.noaa.gov/sst/) , respectively. Daily calculations of turbulent fluxes including wind stress and components, latent and sensible heat fluxes over global ocean at 0.25°×0.25° spatial resolution is perfumed based upon the method described in [SP12]. However, IFREMER product of interest is calculated based on the use of the updated bulk parameterization COARE4.0 [SP20].

## 2.2 HOAPS

Data used in this poject are related to HOAPS-3. Methods, processing, and data are described in details in [SP2] and [SP3] as well as in [WB4]. Briefly, HOAPS-3 contains 6-hourly (swath data) and monthly fields of surface fluxes and related atmospheric parameters over the global ice-free ocean. It also utilizes passive microwave data from the SSM/I instruments to retrieve basic variables. From these individual components of surface fluxes of heat, evaporation, and precipitation are derived. These data as well as the resulting net freshwater flux (E-P) fields are provided on a half degree grid through. HOAPS-3 latent heat flux retrieval is based on the bulk aerodynamics COARE algorithm described [SP62]. This requires atmospheric specific humidity (implemented after (Bentamy et al, 2003)) and sea surface saturation specific humidity (Qs) as well as near surface wind speed (W10). Qs is estimated from sea surface temperature (SST). The latter is derived from the NODC/RSMAS Pathfinder SST data set which uses AVHRR data. The near surface wind speed and the precipitation in HOAPS are directly retrieved from the SSM/I measurements by a neural network approach.

The results shown in this report are derived from the newly daily analyses of HOAPS fluxes. They are calculated from swath retrievals based on the use of space and time interpolation method. The resulting fields are provided by DWD team.

## 2.3 SeaFlux

The SeaFlux are available over global ice free oceans at high space (0.25°×0.25°) and time (3-hourly) resolutions. At our best knowledge, they are the newest flux product processed from remotely sensed data. Data are available from January 1998 through December 2007. Details relied on methods and data may be found in [SP57], and in dedicated website [WB6]. Latent and sensible heat fluxes are estimated based on the use of COARE3.0 bulk parameterization [SP62]. The required wind speed is derived from Cross-Calibrated Multi-Platform (CCMP) Ocean Surface Wind Components data (Atlas et al, 2011). CCMP wind product at 10m is

calculated from cross-calibration and assimilation of wind retrievals from SSM/I, TMI, AMSR-E, QuikSCAT, and SeaWinds onboard ADEOS-2. The retrievals are combined with conventional observations. Variational analysis method (VAM) is used for CCMP wind calculation over global oceans. For VAM starting, ECMWF reanalysis (ERA-40) is used for the period July 1987 – December 1998; The ECMWF operational analysis is used from January 1999 through June 2009. CMMP data are available at synoptic times (00h:00, 06h:00, 12h:00, 18h:00 UTC) with a spatial resolution of 0.25×0.25°. The specific air humidity at 10m and air temperature (Ta) are both retrieved using method described in [SP58]. The method leads to the estimation of Qa10 and Ta based on the use of nonlinear regression algorithm (neural network) to microwave brightness temperatures. The algorithm requires SST information aiming at regularization of the inverse problem. SST required for SeaFlux flux calculation is NOAA SST.

The SeaFlux product is three-hourly (averaged from 0000-0300Z, 0300-0600Z, 0600-0900Z, etc.). All variables are currently available from January 1, 1998 through December 31, 2007.

## 2.4 J-OFURO

Japanese Ocean Flux Data Sets with Use of Remote Sensing Observations (J-OFURO) data set offers global ocean fields of latent and sensible heat fluxes and of the related bulk variables. In this project, J-OFURO version 2 is used. It was recently updated (February 20, 2014). The new version is is referred as HF004 [WB7]. The fluxes are obtained based on version 3 of the COARE bulk algorithm [SP62. The input parameter Qa10 is derived based on F10, F11, F13, and F14 SSM/I Tb using the empirical model (SP58]. Wind speed at 10m is estimated using all available satellite data [SP60] including radiometers such as SSM/I, Aqua/AMSR-E, and TRMM/MI, and scatterometers onboard ERS-1, ERS-2, and QuikSCAT. Air temperature is derived from NCEP-2 re-analysis. Finally, for SST, J OFURO2 uses the new merged multi-satellite and in situ product MGDSST [SP61] constructed by Japan Meteorological Agency (JMA).

Daily and monthly analyses are estimated for turbulent fluxes as well as for bulk variables. Data description may be found in [WB7].

## 2.5 OAFlux

The OAFlux data are available for years 1985-2014 as daily estimates on a 1°× 1° spatial grid [SP43]. OAFlux uses NOAA SST daily [SP47]. The latter have a 0.25° horizontal resolution at daily time scale. In addition to the NOAA SST dataset, OAFlux also utilizes SST values from re-analyses by the ECMWF reanalysis (ERA-40) and from NCEP. The SST data from the re-analyses are re-gridded by WHOI to 1° resolution for ease of synthesis with the Reynolds SST data through objective analysis (used for all surface meteorological variables and fluxes); this analysis is based on the Gauss-Markov approach. For Qa estimation, OAFlux applies the Chou et al. [SP18] algorithm. OAFlux estimation also used values for 2 m specific humidity from the NCEP and ECMWF re-analyses and applied advanced objective analysis to

the inputs. For wind speed, OAFlux uses QuikSCAT and version 6 of the Special Sensor Microwave/Imager (SSM/I) data. The algorithm used to derive the SSM/I data is described in [SP64] . The data used for OAFlux calculation purpose were 12-hourly averaged at a swath resolution of 25 km. Wind speeds were flagged if cloud/rain liquid water values exceeded 18 mg cm-1 because the accuracy of wind speed retrievals degrades if rain is present. Wind speed values were also flagged if measurements are within 50-100 km of the coast or within 200 km of the climatological monthly mean position of the ice edge. In addition to the sources cited, OAFlux also utilizes AMSR-E data as well as data from NCEP and ECMWF re-analyses. A variational method is applied to the data, which is subjective due to the determination of weights. The estimation winds are converted to the equivalent wind speed at 10 m height and to neutral stratification. Air temperatures are from NCEP and ECMWF re-analyses at 2 m height and applied advanced objective analysis to the data; the analysis of air temperature is processed from September 1, 2002 and onward using the ERA-interim reanalysis to replace NCEP. To obtain turbulent fluxes, OAFlux products are calculated based on the use of COARE3 parameterization.

Full details of OAFlux method and products are available at (http://oaflux.whoi.edu/data.html )

## 2.6 ERA Interim

Era-Interim (Simmons et al., 2006) refers to the re-analyses of atmospheric parameters produced by the European Center for Medium Weather Forecasts (ECMWF). It uses 4D-variational analysis on a spectral grid. This re-analysis covers the period from 1989 to the present day. The ERA-Interim data used in this study was obtained from the ECMWF data server on a fixed grid of 0.75°. The main parameters used in this study are specific air humidity and air temperature at 2m, available at synoptic times (00h:00, 06h:00, 12h:00, 18h:00 UTC), converted to Qa10 and to Ta10 , respectively, utilizing the COARE3.0 model [SP62]. The quality of Qa10 and of Ta10 is checked through comparisons with moored buoy (see subsection 1.9) estimates. The main finding of interest for this study is that Era Interim Ta10 are underestimated for buoy Ta10 exceeding 20°C. A bias correction is determined from linear regression between Era Interim and buoy Ta10 estimates.

The dedicated web site for ERA Interim data and documentation is [WB5]

## 2.7 CFSR

NCEP Climate Forecast System Reanalysis (CFSR) [WB10] developed by the US NOAA NCEP. The data used for this study are from the NOAA's National Operational Model Archive and Distribution System (NOMADS), which is maintained by the NOAA's National Climatic Data Center (NCDC) [SP65]. The coupled model consists of a spectral atmospheric model at a resolution of T382 (38km) with 64 hybrid vertical levels and the GFDL Modular Ocean Model. The atmosphere and ocean models are coupled with no flux adjustment. The NCEP-CFSR uses the GSI data assimilation system for the atmosphere. Flow dependence for the background error variances is

included as well as first order time interpolation to the observation Variational quality control of observations [SP66] is also included. An ocean analysis for SST is also performed using Optimal Interpolation (OI). A full range of observations is used as in the other re-analyses which are quality controlled and bias corrected, including satellite radiances. Observations of ocean temperature and salinity are also used.

Details of CFSR data are available in (http://cfs.ncep.noaa.gov/cfsr/)

## 2.8 MERRA

The Modern-Era Retrospective Analysis for Re- search and Applications (MERRA) [SP67]. It is a reanalysis from NASA extending from 1979 to the present. It is routinely used to analyze NASA Earth Observing System (EOS) satellite data as well as conventional observations and operational satellite data in support of NASA science and field missions. [SP68] provides an overview of MERRA. Surface winds are assimilated over the ocean using data from Special Sensor Microwave Imager (SSM/I) and scatterometer retrievals. Sea surface temperature and sea ice are prescribed from the Reynolds dataset (Reynolds et al. 2002). The prognostic variables atmospheric temperature and moisture at the lowest model level are used for computing the vertical gradients in moisture and temperature needed for calculation of the latent and sensible heat fluxes. The planetary boundary layer (PBL) scheme parameterization uses the Lock et al [SP69] and the Louis et al. [SP70] schemes for unstable and stable conditions, respectively. .Neutral transfer coefficients are computed based on standard similarity relationships using a momentum roughness length based on [SP71], a roughness length for heat based on [SP72], and a roughness length for moisture that is a factor of 1.5 larger than the roughness length for heat. 10m height surface humidity and temperature are estimated as diagnostic outputs based on the use of the computed fluxes and transfer coefficients. MERRA data are hourly available at about 0.50° (1/2°) latitude and 0.66° (2/3°) longitude grid points.

## 2.9 NOCS2

The NOCS-2 fluxes (National Oceanography Centre Surface flux dataset version 2) is available daily, gridded at 1°x1° resolution [SP15]. The NOCS fluxes are calculated from in situ observations from Voluntary Observing Ships (VOS), adjusted for known biases, and gridded to provide global coverage using optimal interpolation. Known biases include issues such as: ship heat island effects and changing height of observations due to increases in the mean height of vessels over time for air temperatures; inadequate ventilation of wet bulb thermometers for humidity; changes in observation methods from bucket temperatures to engine room intake or hull sensors for SST; and the influence of anemometers on visual observations and flow distortion due to ship superstructure on wind speeds. All observations are adjusted to 10m reference height, and the bulk formulae of Smith et al [SP73] and [SP74] were used to calculate turbulent fluxes.

## 2.10 Moorings

About 200 moored buoys were collected and investigated prior any use for flux product validation purposes.

High quality bulk variable measurements are derived from OceanSITES buoy network [WB13]. The moorings are an integral part of the Global Ocean Observing System (GCOS). Most of OceanSITES buoys are located in tropical zones of the Atlantic, the Indian, and the Pacific oceans. Only Kuroshio Extension Observatory (KEO) buoys are moored at extra-tropical. The OceanSITES buoy number increases from 7 in 1999 to 37 in 2009.

Turbulent fluxes are calculated from validated hourly buoy 10m wind speed, specific air humidity, and air temperature in combination with sea surface. The adjustment to 10m height of basic variables (W10, Qa, Ta) as well the estimation of turbulent fluxes are performed using COARE4.0 algorithm [SP20].

| Product | W | $Q_a$ | SST | $T_a$ | | LHF | SHF | LW | SW | Period | Spatial Resolution | Temporal Resolution | Format |
|---|---|---|---|---|---|---|---|---|---|---|---|---|---|
| IFREMER | X | X | X | X | X | X | X | | | 1999 – 2009 | 0.25°×0.25° | Daily | NetCdf |
| HOAPS (New release) | X | X | X | X | | X | X | X | X | 1987 - 2008 | 0.5°×0.5° | 6-hourly Daily Monthly | NetCdf |
| OAFLux | X | X | X | X | | X | X | X | X | 1985 - 2014 | 1°×1° | Daily | NetCdf |
| SEAFLUX | X | X | X | X | | X | X | | | 1998 - 2007 | 0.25°×0.25° | 3-hourly | Binary |
| J-OFURO | X | X | | | X | X | X | | | 1988 - 2008 | 1°×1° 0.25°×0.25° | Daily Monthly | NetCdf |
| ERA Interim | X | X | X | X | X | X | X | X | X | 1992 - 2012 | 0.75°×0.75° | 6-hourly | Grib |
| CFSR | X | X | X | X | X | X | X | X | X | 1992 - 2010 | 0.38°×0.38° | 6-hourly | Grib |
| MERRA | X | X | X | X | X | X | X | X | X | 1992 - Present | 0.50°×0.66° | hourly | NetCdf |
| NOCS2 | X | X | X | X | | X | X | | | 1992 – 2010 | 1°×1° | Daily Monthly | NetCdf |

**Table 6: Available flux data meeting WP21 requirements. Data involves bulk variables: 10-m wind speed (W10), 10-m specific air humidity (Qa), sea surface temperature (SST), and 10-m air temperature (Ta), as well as turbulent fluxes: wind stress (?), latent heat flux (LHF), and sensible heat flux (SHF), and radiative fluxes : Long wave (LW), and short wave (SW).**

# 3 Spatial and Temporal Standardizations

Table 6 indicates that flux products are available with various spatial and temporal resolutions. For easier inter-comparisons of flux products at various space and time scales, each product is used to estimate fluxes and the associated parameters as daily fields with the spatial resolution of 0.25° in longitude and latitude over global oceans

## 3.1 Temporal Resolution Issue

As shown above, HOAPS, SeaFlux, are available provided as 6-hourly data over SSM/I swaths and 3 hourly analyses, respectively, while ERA Interim and CFSR are both 6-hourly estimates. Daily HOAPS, SeaFlux, ERA Interim, and CFSR data are estimated at each product grid point (0.50°×0.50°, 0.25°×0.25°, 0.75°×0.75°, 0.38°×0.38°, for HOAPS, SeaFlux, ERA Interim, and CFSR, and respectively). They are calculated as arithmetic averages of available data at each grid point. The quality of daily averaging procedure is sampling dependent. In (OHF progress June 2015) we investigated the impact of the sampling scheme on daily averages estimated from HOAPS data available 6-hourly over SSM/I swaths. In this study, the newly HOAPS data are used. They are provided by DWD team as daily averaged estimates. The latter are calculated based on the use of a spatial and temporal interpolation method. Figure 1 and 2 show monthly mean difference between previous (arithmetic averaging procedure) and new release daily turbulent fluxes (LHF and SHF) for January and July 2000, respectively.

On average, the two HOAPS daily LHF as well as SHF are quite close. Indeed, 99% of LHF and SHF differences are lower than 10W/m² and 5W/m², respectively. The associated RMS differences, calculated from mean and STD differences are lower than 30W/m² and 15W/m² for about 97% of LHF and SHF differences, respectively. Nevertheless, higher differences are depicted along equatorial region. The former tend to meet the rain pattern over this specific region. Figure 1 and 2 do not show any significant seasonal patterns of the differences. Therefore, the results aiming at the characterization of the quality of daily LHF and SHF estimated from HOAPS data and based on the arithmetic averaging procedure should be considered with caution.

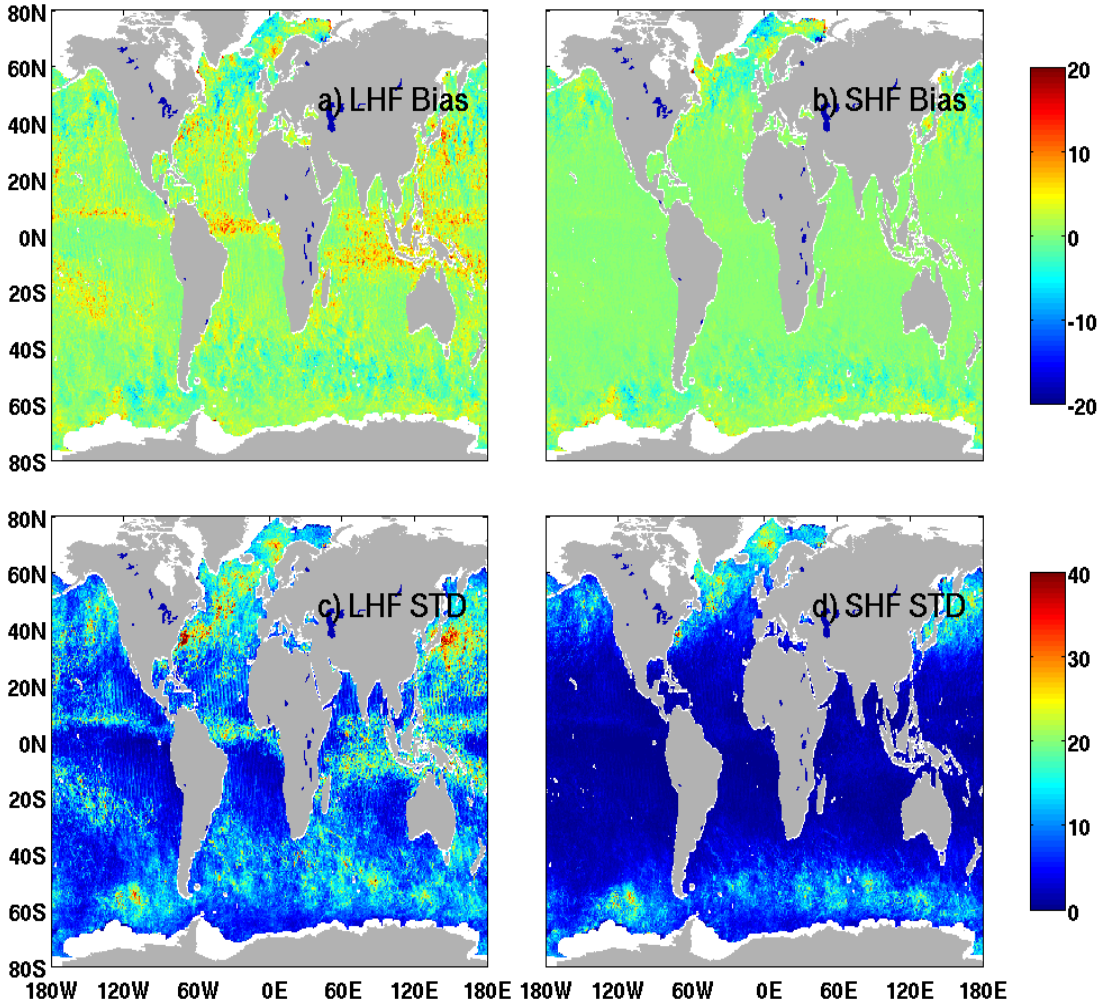


**Figure 1: Spatial distributions of the mean difference (top) and of the associated standard deviation (STD) (bottom) between the daily LHF and between SHF estimated from 6-hourly swath data and from space and temporal objective method for January 2000.**

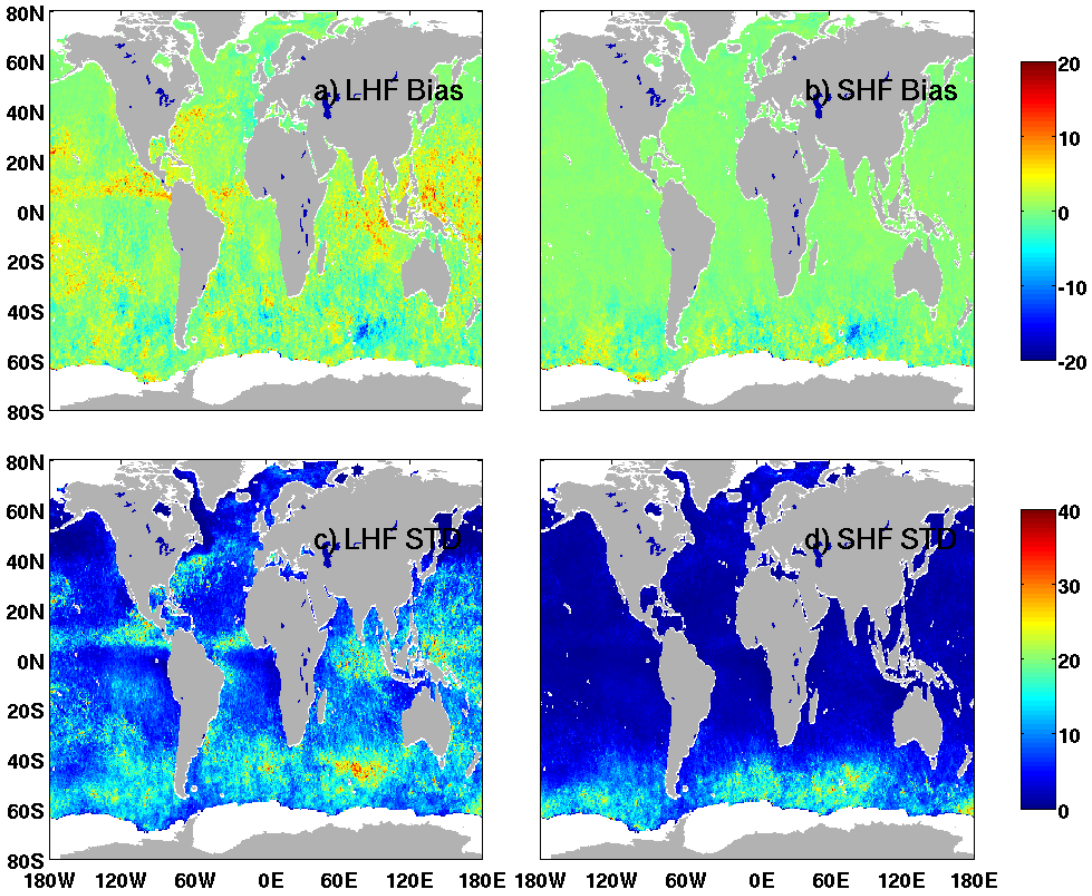


**Figure 2: Spatial distributions of the mean difference (top) and of the associated standard deviation (STD) (bottom) between the daily LHF and between SHF estimated from 6-hourly swath data and from space and temporal objective method for July 2000.**

## 3.2 Spatial Resolution

Each flux product listed in Table 6 is interpolated onto the same regular 0.25° latitude/longitude grid map, based on Spline method. This method is suitable for re-gridding data process.

For each variable (bulk and turbulent variables), namely X, the associated new value, $\widetilde{X}$ , at 0.25°×0.25° grid point is determined as follows:

$$\widetilde{X}(x_i,y_i)=\frac{x_i-x_2}{x_1-x_2}\frac{y_i-y_2}{y_1-y_2}X(x_1,y_1)+\frac{x_i-x_1}{x_2-x_1}\frac{y_i-y_2}{y_1-y_2}X(x_2,y_1)+$$
$$\frac{x_i-x_2}{x_1-x_2}\frac{y_i-y_1}{y_2-y_1}X(x_1,y_2)+\frac{x_i-x_1}{x_2-x_1}\frac{y_i-y_1}{y_2-y_1}X(x_2,y_2) \quad (1)$$

Where xi and yi are $\widetilde{X}$ longitude and latitude coordinates. (xj,yj)j=1,2 are the coordinates of the four closest X of $\widetilde{X}$ location.

This method may induce discontinuities in the resulting gridded fields. However, significant gradient present in the original data should be retrieved.

For each product, valid data available daily and within □h km from a grid point of 0.25°×0.25° are used to estimate the interpolated data (eq. 1). □h values are 25km for IFREMER and SeaFlux, 50km for HOAPS, 100km for OAFlux and J-OFURO, 75km for ARA Interim, and 38km for CFSR.

Example of the interpolation result is shown in Figure 3. It indicates daily HOAPS LHF (left) calculated from original data (see above) and interpolated daily HOAPS LHF (right). As expected most of HOAPS LHF features are also found in the interpolated field.

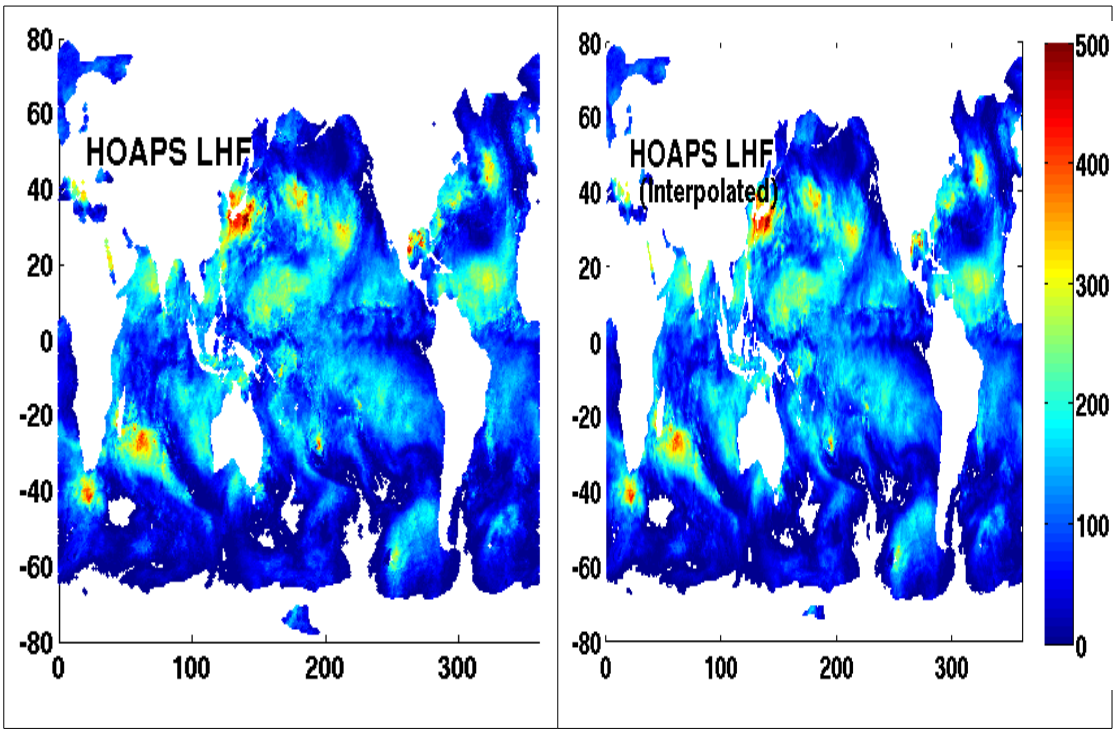


**Figure 3: Daily HOAPS LHF onto original grid (0.50°×0.50°) (left) and onto common grid (0.25°×0.25°) (right) for 1st January 2002.**

## 3.3 Quality Control

This section aims at the assessment of the impact of the space and time interpolation on the resulting flux fields. To avoid any further errors relied on the space and time collocation of the original and interpolated data, the interpolation impact is only investigated based on the comparisons of original and interpolated statistical distributions. Figure 7 and Figure 8 illustrate the distribution comparisons based on the comparison of the statistical quantiles estimated from original and interpolated LHF and SHF data, respectively. Comparisons are shown for IFREMER (Fig. 7a), HOAPS (Fig. 7b), OAFlux (Fig. 7c), SeaFlux (Fig. 7d), J-OFURO (Fig. 7e), and ERA Interim (Fig. 7f). The comparisons are performed for data occurring over global oceans and on 3th January 2000. These examples indicate that the two kinds of LHF and of SHF distributions are comparable for most of variable ranges. As expected, the best agreements are found for the interpolated data estimated from products available with a spatial resolution of 0.25° (IFREMER LHF and SHF, and SeaFlux LHF). Slight departures are found for high values. The associated interpolated estimates tend to be underestimated compared to the original data. The main discrepancy is found for SeaFlux SHF exceeding 200W/m² (0.5% of total data). It is relied on SHF occurring on areas located north of 70°N. These values are retained in the interpolated fields due to the use of a dedicated land and ice masks.

Further controls are performed to assess the quality of the interpolated data. For instance, statistical parameters aiming at the assessment of the comparisons of

original and interpolated LHF and SHF distribution quantiles are calculated for every day of 2000, from data occurring over global oceans as well as over some specific oceanic regions (high latitudes of the Atlantic ocean (55°N – 65°N), Gulf stream, the Atlantic tropical zone (15°S-15°N), and the Mediterranean Sea). The time series of slope of the linear regression between quantiles from original and interpolated data varies between 0.96 and 0.99 for LHF and between 0.95 and 0.98 for SHF. The associated intercepts are lower than 1W/m² for both LHF and SHF.

The quality of the method (1), used for “homogenization” purpose, is checked trough the comparisons of the related results with daily LHF estimates calculated from original data over the grid map of 0.25° in longitude and latitude, but based on a method aiming at the providing smooth interpolation of two dimensional fields. The code and data test are both provided by the OHF expert Dr Sergey Gulev. Figure 8 illustrates the comparison results. It shows daily LHF estimated from original OAFlux over 0.25° grid map based on the two interpolation methods. The two interpolated fields exhibit very similar LHF patterns. No significant differences are depicted. For further investigations, the statistical distributions of the two interpolated LHF data are compared based on the method shown above. The calculation of slopes of the linear regressions between quantiles from the two daily LHF datasets, available for January 2000, are about 0.99, while the associated intercepts are lower than 1W/m².

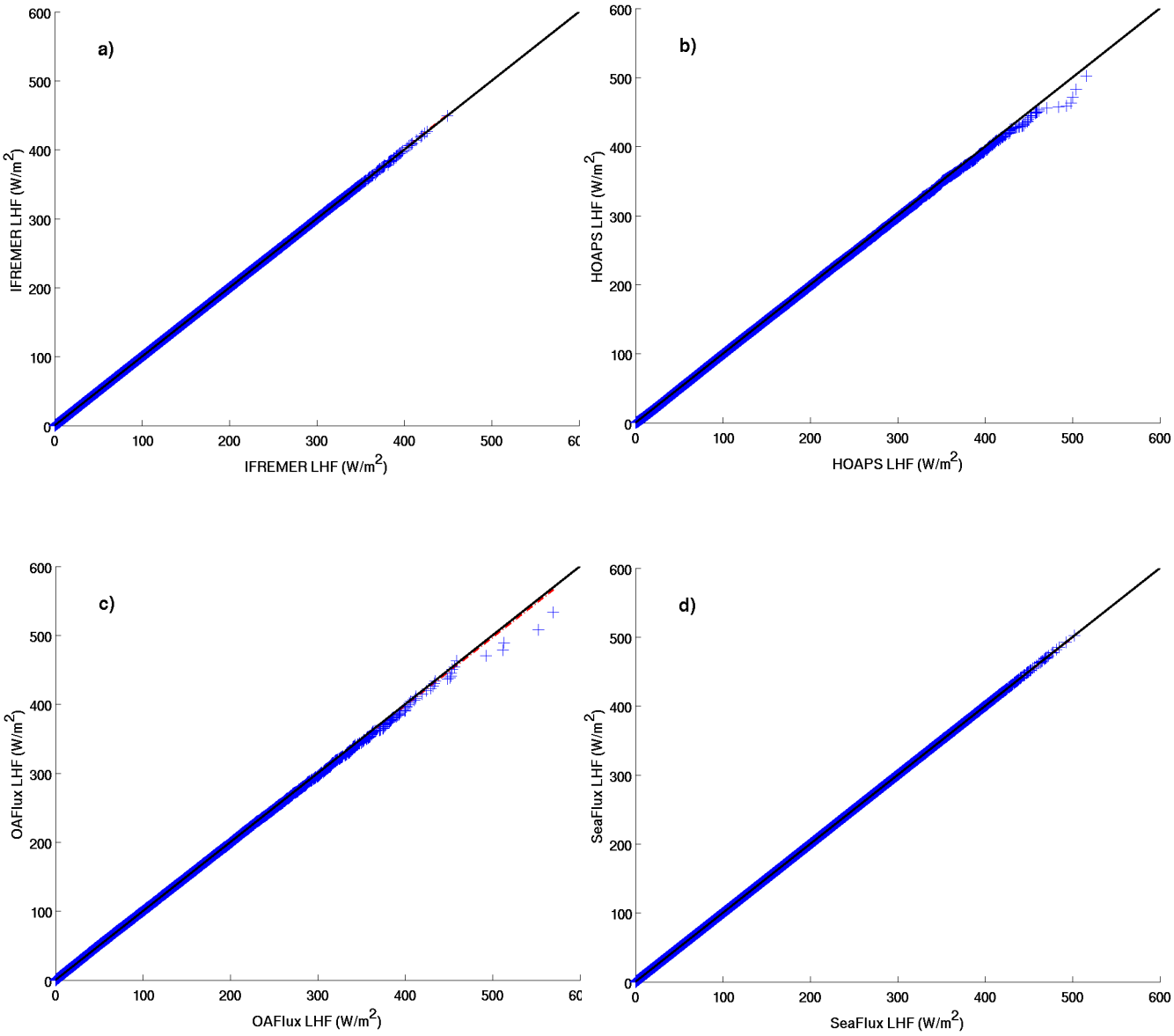
a)
IFREMER LHF (W/m2)
IFREMER LHF (W/m2)
b)
HOAPS LHF (W/m2)
HOAPS LHF (W/m2)
c)
OAFlux LHF (W/m2)
OAFlux LHF (W/m2)
d)
SeaFlux LHF (W/m2)
SeaFlux LHF (W/m2)

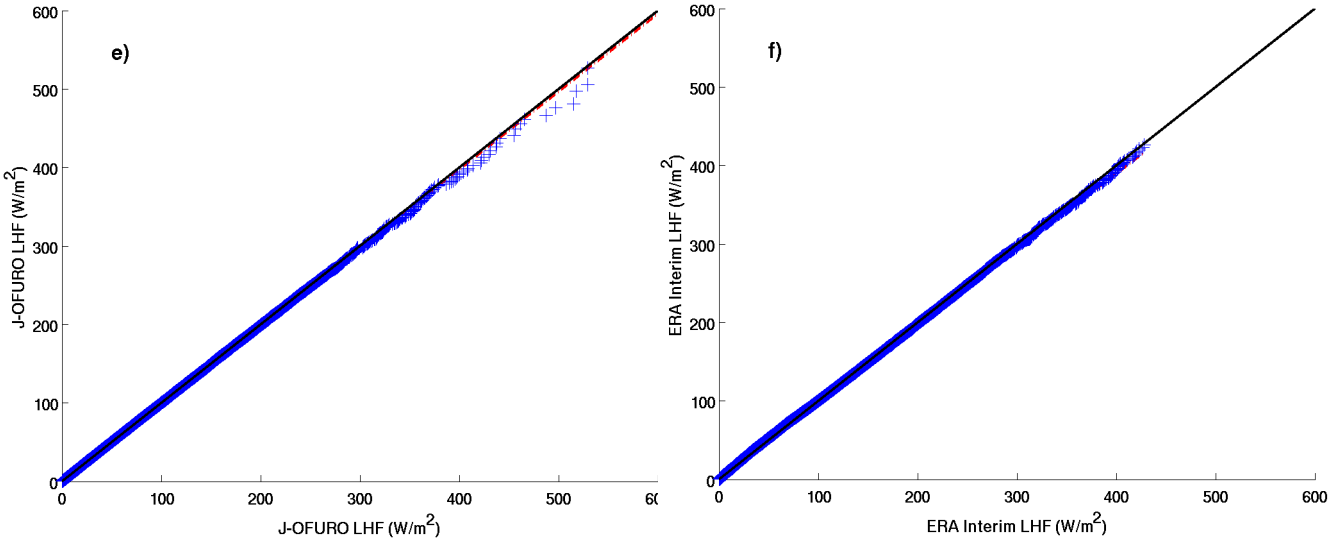


**Figure 4: Comparisons of Original and interpolated LHF from IFREMER (a), HOAPS (b), OAFlux (c), SeaFlux (d), J-OFURO (e), and ERA Interim (f). They are estimated from global data occurring on 3 Jabury 2000.**

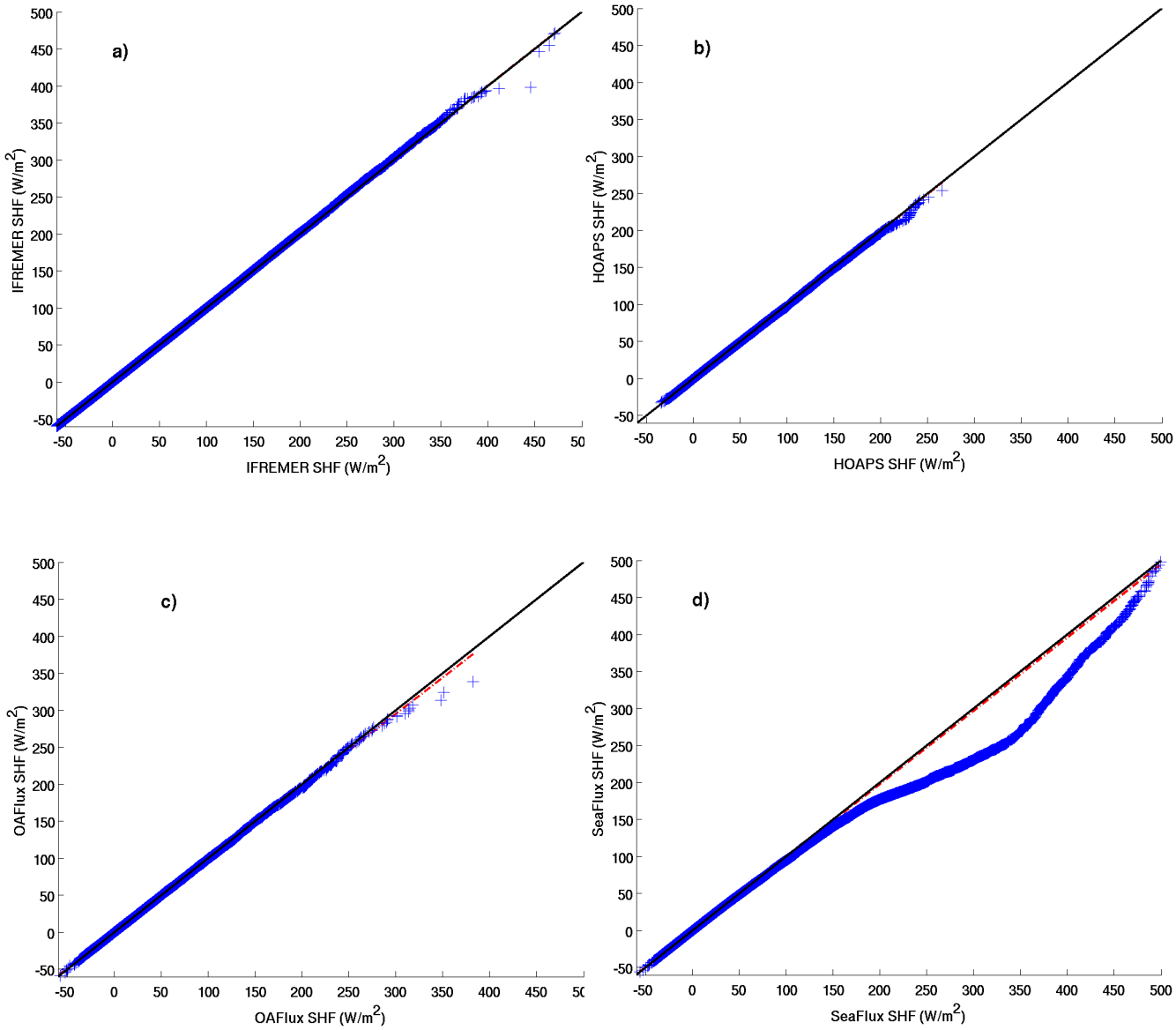
a)
IFREMER SHF (W/m2)
IFREMER SHF (W/m2)
b)
HOAPS SHF (W/m2)
HOAPS SHF (W/m2)
c)
OAFlux SHF (W/m2)
OAFlux SHF (W/m2)
d)
SeaFlux SHF (W/m2)
SeaFlux SHF (W/m2)

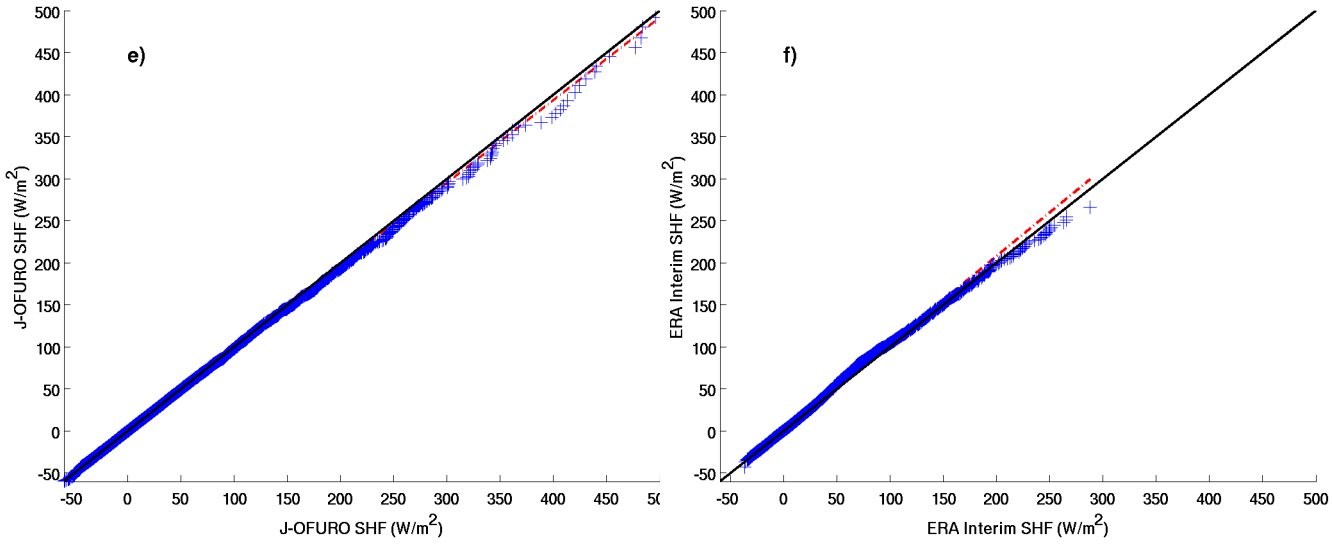


**Figure 5: Comparisons of Original and interpolated SHF from IFREMER (a), HOAPS (b), OAFlux (c), SeaFlux (d), J-OFURO (e), and ERA Interim (f). They are estimated from global data occurring on 3 Jabury 2000.**

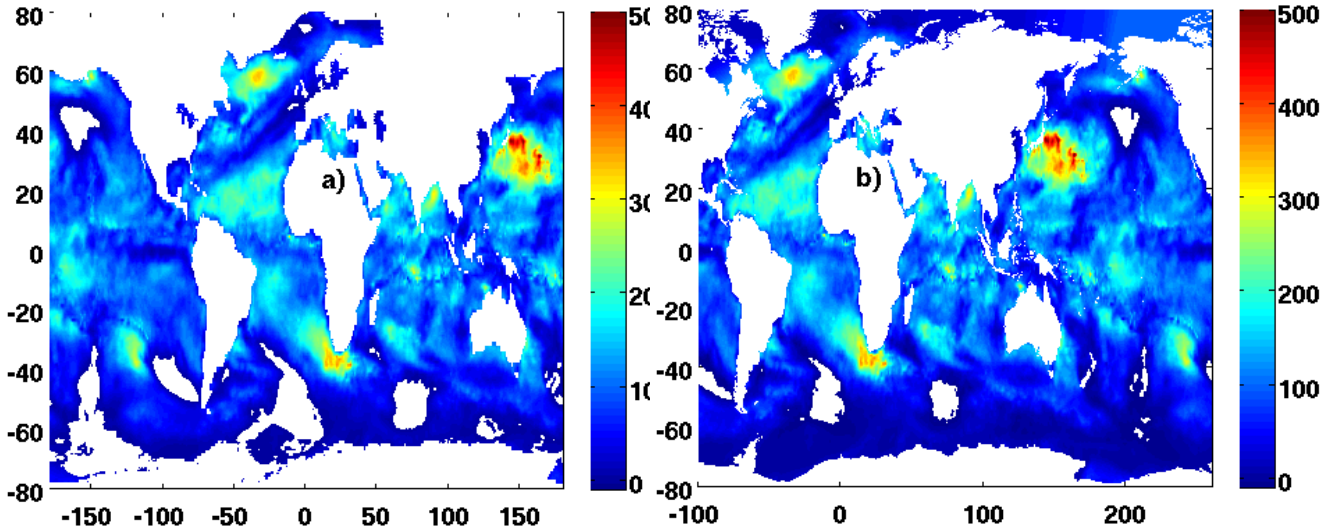


**Figure 6: Interpolated Daily LHF flux calculated based on a) Spline linear method (eq. 1) and on b) the method provided Dr Gulev, from original estimates of 1s January 2000.**

## 3.4 File Format

The “standardized” products are stored using the NetCDF format.

NetCDF (network Common Data Form) is an interface for array-oriented data access and a library that provides an implementation of the interface. The NetCDF library also defines a machine-independent format for representing scientific data. Together, the interface, library, and format support the creation, access, and sharing of scientific data. The NetCDF software was developed at the Unidata Program Center in Boulder, Colorado. The NetCDF libraries define a machine-independent format for representing scientific data.

Example of file structure is shown hereafter for IFREMER product:

**Source**:

```
ifremerflux-20000103120000-OHF-L4-global_daily_0.25x0.25-v0.5-
f01.0.nc
```

**Format**:

```
dimensions:
        time = UNLIMITED ; // (1 currently)
        lat = 720 ;
        lon = 1440 ;
variables:
        double lat(lat) ;
                lat:_FillValue = 9.96920996838687e+36 ;
                lat:long_name = "latitude" ;
                lat:standard_name = "latitude" ;
                lat:units = "degrees_north" ;
        double lon(lon) ;
                lon:_FillValue = 9.96920996838687e+36 ;
                lon:long_name = "longitude" ;
                lon:standard_name = "longitude" ;
                lon:units = "degrees_east" ;
        double time(time) ;
                time:_FillValue = 9.96920996838687e+36 ;
                time:long_name = "time" ;
                time:standard_name = "time" ;
                time:units = "days since 1970-01-01 00:00:00Z" ;
        double sea_surface_temperature(time, lat, lon) ;
                sea_surface_temperature:_FillValue = 1.e+20 ;
                sea_surface_temperature:long_name = "sea surface temperature" ;
                sea_surface_temperature:units = "degree Kelvin" ;
        double surface_downward_eastward_stress(time, lat, lon) ;
                surface_downward_eastward_stress:_FillValue = 1.e+20 ;
```

```
                surface_downward_eastward_stress:long_name = "U-component of Surface Wind
Stress" ;
                surface_downward_eastward_stress:units = "Pa" ;
        double surface_upward_latent_heat_flux(time, lat, lon) ;
                surface_upward_latent_heat_flux:_FillValue = 1.e+20 ;
                surface_upward_latent_heat_flux:long_name = "Surface Flux of Latent Heat" ;
                surface_upward_latent_heat_flux:units = "W m-2" ;
        double air_temperature(time, lat, lon) ;
                air_temperature:_FillValue = 1.e+20 ;
                air_temperature:long_name = "air temperature" ;
                air_temperature:units = "degree Celsius" ;
        double eastward_wind(time, lat, lon) ;
                eastward_wind:_FillValue = 1.e+20 ;
                eastward_wind:long_name = "u-component of wind" ;
                eastward_wind:units = "m.s-1" ;
        double northward_wind(time, lat, lon) ;
                northward_wind:_FillValue = 1.e+20 ;
                northward_wind:long_name = "v-component of wind" ;
                northward_wind:units = "m.s-1" ;
        double air_surface_specific_humidity(time, lat, lon) ;
                air_surface_specific_humidity:_FillValue = 1.e+20 ;
                air_surface_specific_humidity:long_name = "Specific humidity" ;
                air_surface_specific_humidity:units = "g.kg-1" ;
        double wind_speed(time, lat, lon) ;
                wind_speed:_FillValue = 1.e+20 ;
                wind_speed:long_name = "wind speed module" ;
                wind_speed:units = "m.s-1" ;
        double surface_downward_northward_stress(time, lat, lon) ;
                surface_downward_northward_stress:_FillValue = 1.e+20 ;
                surface_downward_northward_stress:long_name = "V-component of Surface Wind
Stress" ;
                surface_downward_northward_stress:units = "Pa" ;
        double surface_upward_sensible_heat_flux(time, lat, lon) ;
                surface_upward_sensible_heat_flux:_FillValue = 1.e+20 ;
                surface_upward_sensible_heat_flux:long_name = "Surface Flux of Sensible Heat" ;
                surface_upward_sensible_heat_flux:units = "W m-2" ;
        double wind_stress(time, lat, lon) ;
                wind_stress:_FillValue = 1.e+20 ;
                wind_stress:long_name = "wind stress module" ;
                wind_stress:units = "Pa" ;

// global attributes:
                :Conventions = "CF-1.6, Unidata Observation Dataset v1.0" ;
                :netcdf_version_id = "4.1.1 of Nov  7 2011 11:35:16 $" ;
                :date_created = "20150901T155156Z" ;
                :date_modified = "20150901T155156Z" ;
                :id = "FP1" ;
                :naming_authority = "fr.ifremer.cersat" ;
                :Metadata_Conventions = "Unidata Dataset Discovery v1.0" ;
                :standard_name_vocabulary = "NetCDF Climate and Forecast (CF) Metadata
Convention" ;
                :institution = "Ifremer/Cersat, ESA" ;
```

```
                    :institution_abbreviation = "ifremer/cersat" ;
                    :title = "IFREMER remote sensed flux product" ;
                    :summary = "" ;
                    :cdm_data_type = "grid" ;
                    :keywords = "Oceans > Ocean Flux" ;
                    :keywords_vocabulary = "NASA Global Change Master Directory (GCMD) Science
Keywords" ;
                    :scientific_project = "(OHF) OCEAN-HEAT-FLUX [ESA]" ;
                    :acknowledgement = "" ;
                    :license = "" ;
                    :format_version = "" ;
                    :processing_software = "Cersat/Cerbere 1.0" ;
                    :product_version = "" ;
                    :uuid = "" ;
                    :processing_level = "L4" ;
                    :history = "" ;
                    :publisher_name = "ifremer/cersat" ;
                    :publisher_url = "http,//cersat.ifremer.fr" ;
                    :publisher_email = "cersat@ifremer.fr" ;
                    :creator_name = "" ;
                    :creator_url = "" ;
                    :creator_email = "" ;
                    :references = "" ;
                    :metadata_link = "" ;
                    :source = "" ;
                    :source_version = "" ;
                    :platform = "" ;
                    :platform_type = "" ;
                    :sensor = "" ;
                    :sensor_type = "" ;
                    :band = "" ;
                    :spatial_resolution = "" ;
                    :geospatial_lat_min = -90. ;
                    :geospatial_lat_max = 89.75 ;
                    :geospatial_lat_units = "degrees" ;
                    :geospatial_lat_resolution = 0.25 ;
                    :geospatial_lon_min = -180. ;
                    :geospatial_lon_max = 179.75 ;
                    :geospatial_lon_units = "degrees" ;
                    :geospatial_lon_resolution = 0.25 ;
                    :geospatial_vertical_min = "" ;
                    :geospatial_vertical_max = "" ;
                    :geospatial_vertical_units = "meters above mean sea level" ;
                    :geospatial_vertical_positive = "up" ;
                    :time_coverage_start = "19700101T000000Z" ;
                    :time_coverage_end = "19700101T000000Z" ;
                    :time_coverage_resolution = "daily" ;
                    :source_dataset = "ifremerflux converted to OHF standard format" ;
                    :technical_support_contact = "cersat@ifremer.fr" ;
}
```

# 4 Verification

This section aims at the examination of the quality of the standardized products. It is performed through the comparisons of statistical parameters characterizing the difference between daily in-situ and original product fluxes and between in-situ and standardized products.

The assessment of the product quality is performed through the comparisons with daily latent and sensible heat fluxes estimated from OceanSites measurements. The collocated daily buoy and product data, required for comparison purpose, are determined based on the spatial criteria, distance separating buoy and product, are less than the product spatial resolutions. Obviously, the space criterion is same for all standardized products. The statistics results characterizing the comparisons are summarized in Table 7. They indicate that statistics relied on standardized products meet those estimated for original products. For instance both original and standardized IFREMER LHF estimates tend to be slightly overestimated compared to OceanSites estimates, whereas OAFlux and SeaFlux LHF estimates are slightly underestimated. The associated standard deviation, correlation coefficients, and symmetrical coefficients values calculated for original and standardized data are close. Similar results are found for the comparisons between statistical parameters characterizing the difference between moorings and original SHF products and between buoys and standardized products.

| Statistic Parameters | Product | LHF | | SHF | |
|---|---|---|---|---|---|
| | | Original | Standardized | Original | Standardized |
| Bias | IFREMER | -2.20 | -3.34 | 0.09 | -0.63 |
| | HOAPS | -5.25 | -3.76 | -1.27 | -0.64 |
| | OAFlux | 4.26 | 1.76 | 1.31 | 0.65 |
| | SeaFlux | 7.63 | 7.76 | -1.93 | -1.76 |
| | J-OFURO | 1.29 | 0.98 | 2.27 | 1.86 |
| | ERA Int | -12.01 | -13.67 | -2.42 | -2.14 |
| Standard deviation | IFREMER | 30.03 | 28.16 | 7.16 | 6.75 |
| | HOAPS | 42.21 | 41.21 | 9.63 | 9.63 |
| | OAFlux | 31.49 | 29.42 | 5.49 | 4.96 |
| | SeaFlux | 30.93 | 30.16 | 6.73 | 6.47 |
| | J-OFURO | 36.31 | 34.67 | 7.19 | 6.56 |
| | ERA Int | 27.34 | 27.00 | 5.55 | 5.11 |
| Correlation | IFREMER | 0.87 | 0.88 | 0.91 | 0.90 |
| | HOAPS | 0.81 | 0.83 | 0.75 | 0.78 |
| | OAFlux | 0.87 | 0.89 | 0.92 | 0.92 |
| | SeaFlux | 0.88 | 0.88 | 0.88 | 0.88 |
| | J-OFURO | 0.85 | 0.86 | 0.86 | 0.87 |
| | ERA Int | 0.90 | 0.90 | 0.92 | 0.93 |
| Regression Symmetric coefficient | IFREMER | 0.83 | 0.83 | 1.15 | 1.14 |
| | HOAPS | 1.12 | 1.06 | 1.14 | 1.08 |
| | OAFlux | 0.88 | 0.86 | 0.95 | 0.99 |
| | SeaFlux | 0.94 | 0.94 | 0.98 | 0.99 |
| | J-OFURO | 1.02 | 1.01 | 0.96 | 0.99 |
| | ERA Int | 0.94 | 0.92 | 0.99 | 0.99 |

**Table 7: Statistics characterizing the comparisons between OceanSites and product (original and standardized) daily fluxes. They are calculated for latent**

**heat flux (LHF in W/m²), and sensible heat flux (SHF in W/m²). Statistics are calculated for each product when available during the associated time interval of 1999-2009 period. Statistics relied on standardized products are calculated for 1999 – 2007 period.**

Further investigations of the standardized flux product quality are performed at some specific OceanSites locations for daily time scales. The moorings located at mid-latitude of the Atlantic Ocean (50°N-145°W), within Kuroshio current (32°N-144.5°E), at extra-tropical zone of the Atlantic Ocean (20°N-38°W), eastern (0°N-170W) and western (0°N-165°E) equator zones of the Pacific Ocean are selected. These locations are assumed illustrating the main known LHF and SHF daily variability at daily scale. Figure7 provides examples of time series of daily LHF estimates for the period December 2007 – January 2008, respectively. For clarity, only buoy, IFREMER and OAFlux are shown. For each product and at each location, the original and standardized data are compared. The related statistics indicate that the two kinds of products are highly correlated. Indeed, most of correlation coefficients exceed 0.98 and the associated symmetrical coefficients are close to 1. The best statistics are found for IFREMER and SeaFlux available on a grid map (Table 1) similar to standardized product map of 0.25° in longitude and latitude. Their correlation as well as their and symmetrical coefficients are very close of 1 at all locations. The mean differences between original and standardized products do not lead to any systematic bias. For instance, most of biases of LHF differences do not exceed 1W/m². However, LHF biases calculated at 32°N-144.5°E for OAFlux and J-OFURO exhibit high values reaching 7W/m² and 9W/m², respectively. At this specific location, LHF experiences high values as well as high space and time variability (Figure 7). For instance, the mean time and STD of LHF calculated from OceanSites buoy time series at this location are about 150W/m² and 103W/m², respectively. Furthermore, 25% and 5% of daily LHF estimates exceed 200W/m² and 350W/m², respectively. Obviously, interpolating such kind of data available at a grid point of 1°×1° (e.g. OAFlux) onto a grid map of 0.25°×0.25°, based on the method shown above (sub-section 2.2), may lead to some departure between original and standardized products.

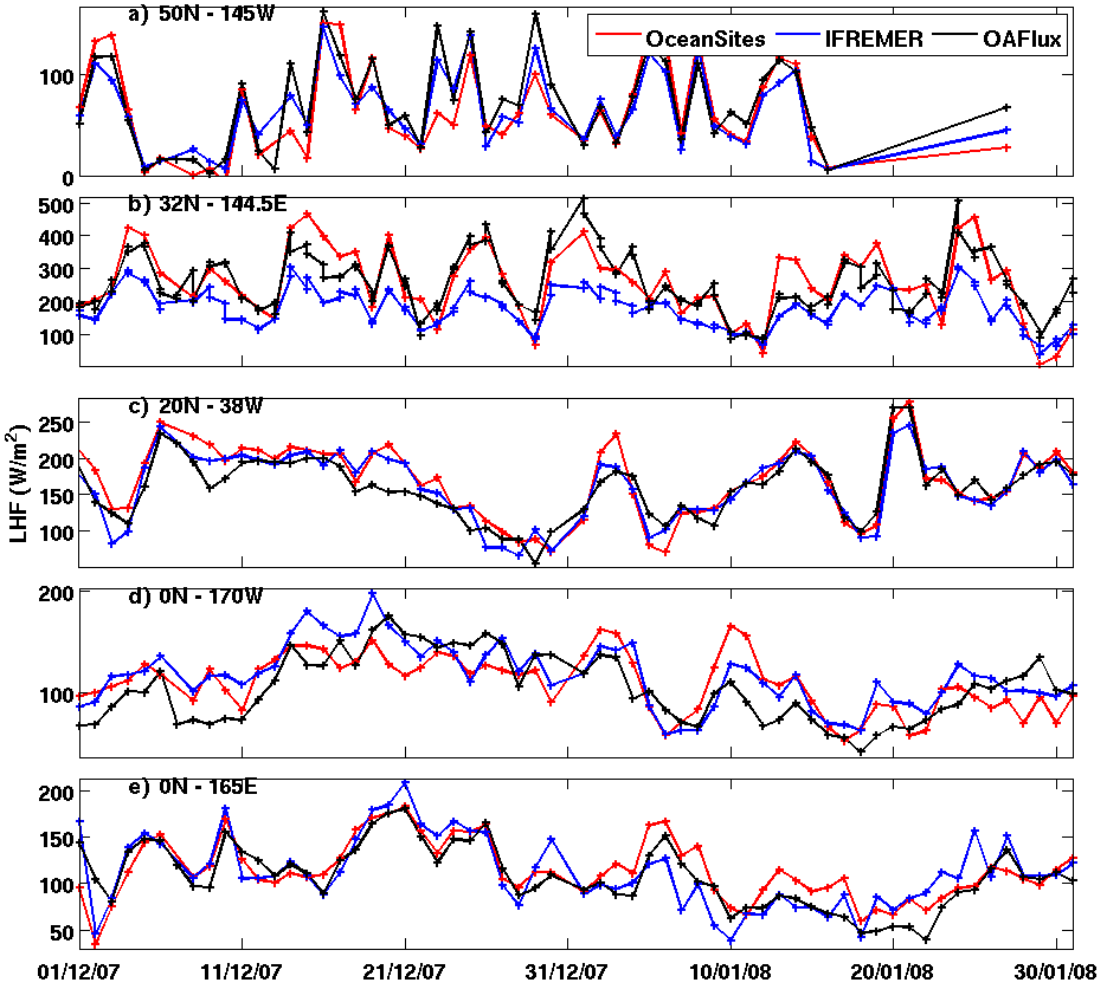


**Figure 7: Time series of daily LHF estimates from OceanSites buoys (in red), IFREMER (blue), and OAFlux (black) at locations a) 50°N-145°W, b) 32°N-144.5°E, c) 20°N-38°W, d) 0°N-170W, and e) 0°N-165°E for the period December 2007 – Januarys 2008.**

# 5 Standardized product patterns

The quality of the resulting standardized flux products is also investigated trough the inter-comparisons of their spatial and temporal patterns. To further assess the pattern comparisons, daily NOCS fluxes are also used (Table 1). Therefore, only collocated in space and time of standardized and NOCS2 data are used for inter-comparison purposes. Figure 8 shows the latitudinal behaviors of the standardized and NOCS2 LHF (Figure 8a) and SHF (Figure 8b) products estimated over the Atlantic Ocean between 55°S and 55°N, and for the period 2003 – 2005. All standardized LHF as well SHF exhibit similar latitudinal behaviors. The latter meet those derived from NOCS2 except in southern ocean where NCOS2 sampling is quite poor. The main known features of LHF and SHF are retrieved from standardized products. However, significant magnitude differences are depicted.

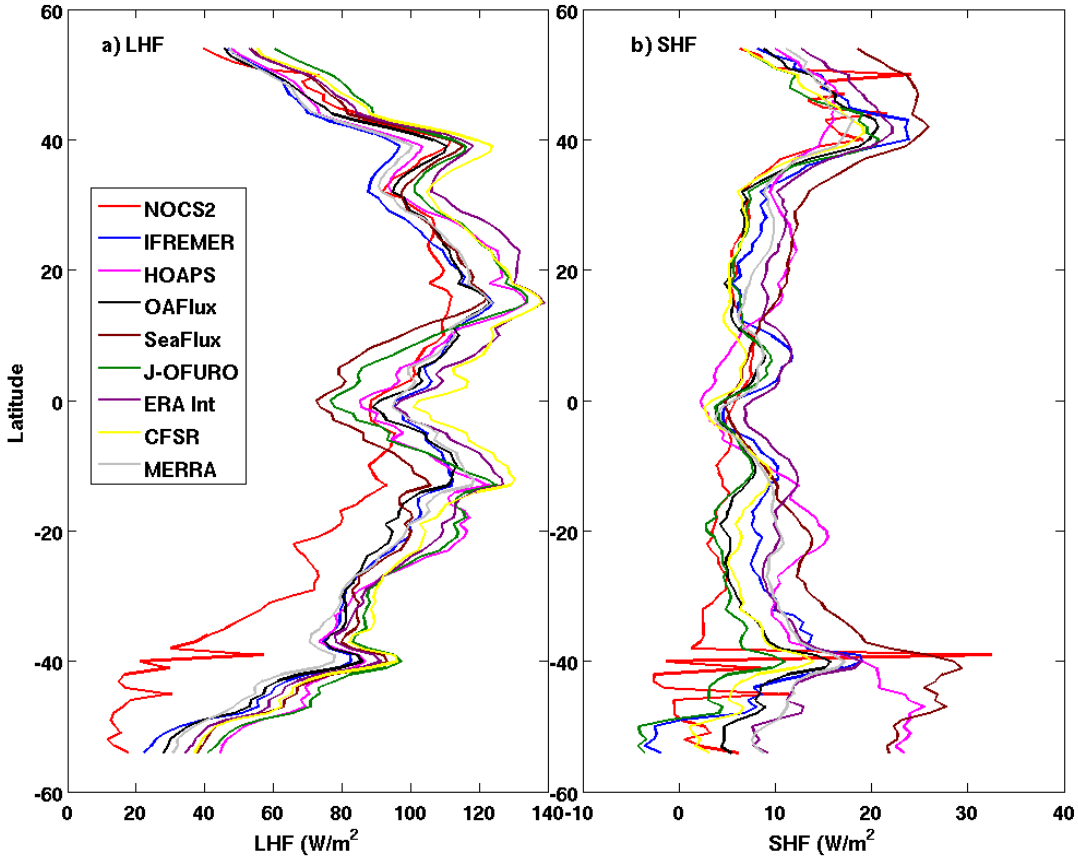


**Figure 8: Latitudinal mean of daily standardized and NOCS LHF (a) and SHF(b) estimated over the Atlantic oceanic basin for the period 2003 – 2005.**

# 6 Regional constraint data for the cage study

This section describes the data generated by OHF project for the cage study.

## 6.1 Estimates of ocean heat content

Global Ocean Heat Content (OHC) derived from in situ observations are a useful benchmark for ocean and climate models and an important diagnostic for changes in the Earth's climate system (Hansen et al., 2005; Levitus et al., 2005). Due to its global coverage, Argo opens up a new scope to observe climate related changes and allows a monitoring of the state of the global ocean through OHC estimates (Figure 9). OHC is defined here as the deviation from a reference period (2005-2012) and is calculated as the integral of $\rho c_p T'(z)dz$ between two depth layers (e.g. surface to 1500m depth) where T' is the temperature anomaly relative to a given climatology. Units of OHC are $J/m^2$.

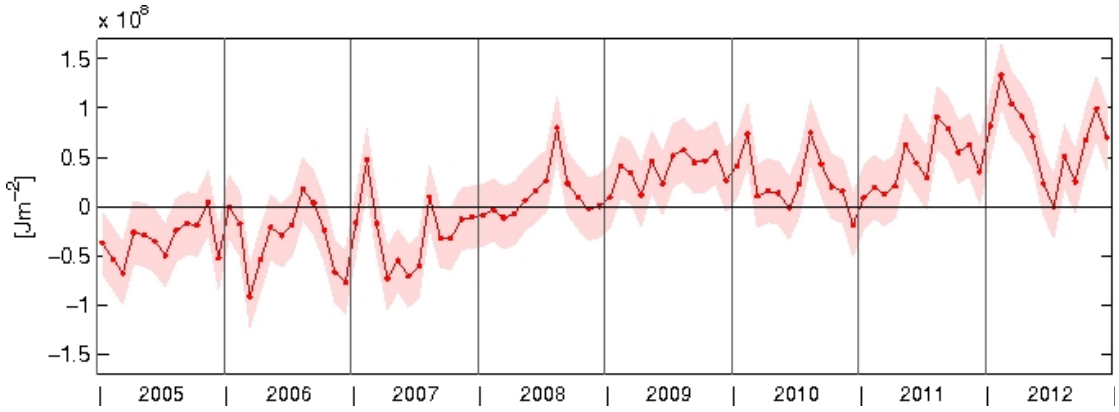


**Figure 9: Times series of global mean ocean heat content (OHC) anomaly relative to the 2005-2012 climatology field for the 10-1500m depth layer and between 60°S-60°N. Global mean OHC has been calculated after the method of von Schuckmann and Le Traon (2011) using measurements from the global Argo observing system. Shaded area indicates the uncertainies of global mean OHC anomalies.**

In the study of von Schuckmann and Le Traon (2011), a method of evaluating OHC is developed that is easy to implement and can be used for a routine monitoring of the global ocean. With this method, a simple estimation of the errors on OHC estimations can be established and thus adequate interpretations and conclusions can be drawn. An Argo climatology (ACLIM hereinafter, 2005–2012, von Schuckmann et al., 2009) is first interpolated on every profile position in order to fill gappy profiles at depth of each temperature profile. This procedure is necessary to calculate depth-integrated quantities. OHC is then calculated at every Argo profile position. Finally, anomalies of the physical properties at every profile position are calculated relative to ACLIM.

To estimate GOIs from the irregularly distributed profiles, the global ocean is divided into boxes of 5° latitude, 10° longitude and 3 month size. This provides a sufficient number of observations per box. To remove spurious data, measurements which depart from the mean at more than 3 times the standard deviation are excluded. The variance information to build this criterion is derived from ACLIM. This procedure excludes about 1% of data. Only data points which are located over bathymetry deeper than 1000m depth are then kept. Boxes containing less then 10 measurements are considered as a measurement gap.

The mean for each 5°×10°×3 month box is then estimated using a weighted averaging method based on the analysis of Bretherton et al. (1976). We chose to replace gaps by the spatial mean. We do take into account, however, the impact of gaps on the error estimation. Finally, OHC is calculated within 60°S to 60°N, i.e. the effective coverage of the Argo array (Roemmich and Gilson, 2009) by averaging the OHC box values weighted by their surface area.

The total error includes the uncertainties due to the data processing and the choice of the reference climatology (see von Schuckmann and Le Traon, 2011 for more details), but it does not take into account possible unknown systematic measurement errors not precisely corrected for in the delayed mode Argo quality control (e.g. pressure errors, salinity sensor drift).

This method can be used, however, to discuss sampling issues for the estimation of OHC and its errors. Uncertainties due to data processing and the climatology of global mean OHC during 2005 and 2012 for different time averages account for 0.52/0.42 J/m2*108 (2005/2012) for 3 month time average, 0.26/0.21 J/m2*108 (2005/2012) for 1 year average and 0.15 J/m2 108 for the 8 year average.

These results show that errors clearly decrease with the growing coverage of Argo. Assuming that the current Argo sampling is sustained for 15 yr, trends of OHC could be performed with an accuracy of about ± 0.02Wm−2 for global OHC.

The results show a clear increase of GOHC (Figure 1). Estimations of uncertainties reveal that this increase is significant during the years 2005–2012. GOHC increases during this period by a rate of 0.5±0.1Wm−2. These time series are regularly distributed to the European Environment Agency (Christiansen et al., 2012), and the international Climate Data Guide (https://climatedataguide.ucar.edu/). Moreover, these OHC estimations have been used to give a first decadal estimation of the Earth's energy imbalance during the Argo era (Hansen et al., 2011, see Figure 10), and they have lead to important discussions for climate change studies (e.g. Trenberth et al., 2010; Balmaseda et al., 2013).

## 6.2 Validation of OHC method

Nevertheless, uncertainties of the Argo ocean observing system, sampling issues, and systematic biases still causes significant spread among the more recent estimates of OHC (Abraham et al., 2013; von Schuckmann and Le Traon, 2011). In

particular, the detection of systematic biases represents a significant challenge for the Argo community, as they are associated with a coherent signature over large areas and are difficult to identify with current regional quality control procedures. Moreover, this type of error has a potentially large impact on Argo OHC estimations (Willis et al., 2009; Barker et al., 2011). The comparison of Argo OHCs to other global ocean observing systems such as total sea level from altimetry, and ocean mass observations from satellite gravimetry via the global sea level budget (e.g., Willis et al., 2008; Leuliette andWillis, 2011) is not only a potential quality control method to identify systematic biases in the Argo observing system, but also to test the effect of Argo sampling issues on OHC estimations.

In the study of von Schuckmann et al. (2014) the Argo steric time series for the global and for different ocean sectors are used to assess the consistency with ocean mass from gravimetry and total sea level from altimetry via the global sea level budget. This is done to investigate whether systematic biases can be detected in the current Argo network, to better understand the impact of Argo sampling for OHC estimations, and to quantify if deep ocean changes below Argo maximum depth can be inferred via the residual global sea level budget.

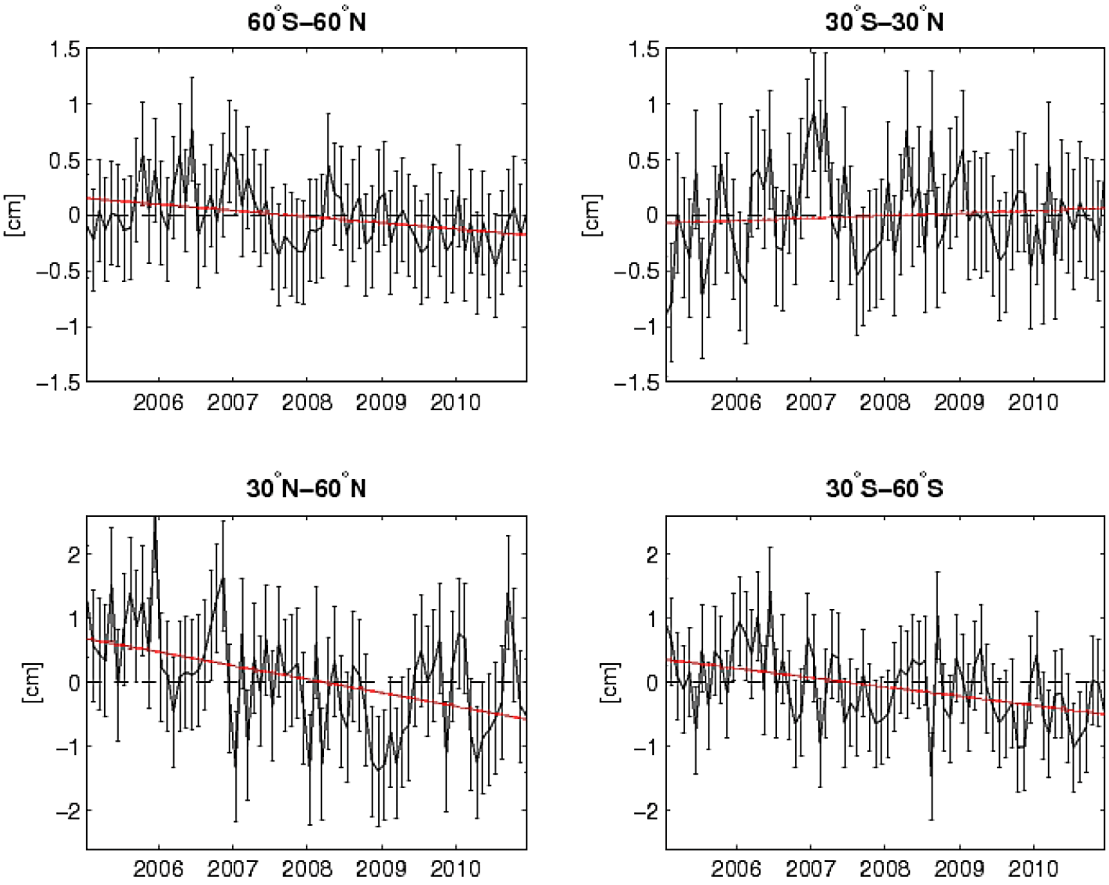


**Figure 10: Residual of the sea level budget at different latitude bands using Argo steric sea level, AVISO delayed mode gridded fields (using subsampled Altimeter data to quantify biases owing to Argo sampling) and GRACE data. Residual trends amount to −0.6±0.6 mmyears−1 for the global ocean, 0.2±0.7 mmyears−1 for the Tropical Ocean, −2.1±0.9 mmyears−1 for the Northern Ocean, and −1.5±0.7 mmyears−1 for the Southern Ocean.**

Sea level change $SL_{TOTAL}$ is related to steric height time series ($SL_{STERIC}$) and mass variability ($SL_{MASS}$) through

$$SL_{TOTAL} = SL_{MASS} + SL_{STERIC} + SL_{RES}, \quad (1)$$

where SL represents sea level (e.g., Willis et al., 2008; Leuliette and Miller, 2009). The residual of the sea level budget ($SL_{RES}$) includes deep-ocean steric changes below 1500m depth (i.e., depth range deeper than what we consider in our analysis of Argo), plus any source of uncertainty in observations and/or data treatment.

To estimate the residual, $SL_{RES}$ three major global observing systems are used: $SL_{TOTAL}$ is computed from altimetry products, $SL_{MASS}$ from satellite gravimetry, and $SL_{STERIC}$ in the upper 1500 m from temperature and salinity observations from Argo (see von Schuckmann et al., 2014 for more details). The error bar of $SL_{RES}$ is derived from the residual sum of squares of the errors of the three time series, assuming that they are independent. Trends of $SL_{RES}$ are calculated using a weighted least square fit, taking into account the error bar of the time series as described in the appendix of

von Schuckmann and Le Traon (2011). Unless otherwise stated, the error bars reflect one standard error and account for the standard error in the fit, the GIA error from GRACE, and the drift error for altimetry. A more detailed description can be found in von Schuckmann et al. (2014).

Our findings show that although both the large regional variability and the uncertainties in the current observing system prevent us from extracting indirect information regarding deep-ocean changes, the global and regional budgets can be closed within error bars (Figure 10). Issues still remain in the extra-tropics. This emphasizes the importance of continuing sustained effort in measuring the deep ocean from ship platforms and by beginning a much needed automated deep-Argo network.

In summary, a method of OHC estimation has been developed which has been validated through the method of physical budget constraints. The OHC method is easy to implement and can be used to develop a validation framework for the OHF project in the context of regional budget constraints (concept of cages). Indeed, results of Figure 2 emphasizes that uncertainties still remain in the extra-tropics, and large discussions and scientific analysis are under the way to understand these discrepancies. Some of these discrepancies have been related to a systematic bias detected in the Altimeter product (Dieng et al., 2015), and others are still under discussion to be related to missing measurements of the deep ocean below 2000m depth. However, in the context of the “concept of cages”, the OHC estimate from Argo can be seen as the most precise reference dataset for the OHF project validation approach.